Scilight

Sustainable Engineering Novit

https://www.sciltp.com/journals/sen

Review

Check for updates

Hydrogel-Based Iontronic Sensing

Weijun Li [1,†], Shihao Wang [1,†], Yigang Shen [2,3,*], Jing Liu [4,*] and Jian Zhang [5,*]

[1] Fujian Key Laboratory of Functional Materials and Application, School of Materials Science and Engineering, Xiamen University of Technology, Xiamen 361024, China
[2] Institute of Precision Machinery and Smart Structure, College of Engineering, Zhejiang Normal University, Jinhua 321004, China
[3] School of Engineering, Cardiff University, Cardiff CF24 3AA, UK
[4] School of Mechanics and Construction Engineering, Jinan University, Guangzhou 510632, China
[5] State Key Laboratory of Bioinspired Interfacial Materials Science, Suzhou Institute for Advanced Research, University of Science and Technology of China, Suzhou 215123, China
* Correspondence: yigangshen@zjnu.edu.cn (Y.S.); jingliu@jnu.edu.cn (J.L.); jianzhang@ustc.edu.cn (J.Z.)
† These authors contributed equally to this work.

How To Cite: Li, W.; Wang, S.; Shen, Y.; et al. Hydrogel-Based Iontronic Sensing. *Sustainable Engineering Novit* **2026**, *2*(2), 1. https://doi.org/10.53941/sen.2026.100006

Received: 30 January 2026
Revised: 8 April 2026
Accepted: 14 April 2026
Published: 28 April 2026

Abstract: Hydrogel-based iontronic sensing (HBIS) is emerging as a compelling frontier at the interface of soft matter, electrochemistry, and bioelectronics, driven by the unique ability of hydrogels to communicate with living systems through hydrated ionic networks rather than electronic conduction in rigid solids. This ionic mode of signal transduction enables intrinsically compliant interactions with biological tissues, electrolytes, and dynamic fluidic microenvironments, making HBIS highly attractive for flexible bioelectronics. As the field evolves from material optimization toward integrated and intelligent systems, a unifying understanding of material design, ion transport, and device function remains lacking. Here, a multiscale quantitative framework is established to bridge structure, transport, and sensing performance in HBIS. Representative material platforms, including polyelectrolytes, ionogels, and nanocomposite hydrogels, are examined alongside key transport mechanisms, such as diffusion, electromigration, convection, electroosmotic flow, adsorption-site hopping, and Grotthuss-type conduction. Quantitative modeling approaches based on electrochemical impedance spectroscopy and Poisson-Nernst-Planck theory are further highlighted, together with emerging applications in iontronic skins, soft robotics, human-machine interfaces, and energy conversion. This review provides a design blueprint for next-generation hydrogel iontronic sensors with improved predictability, adaptability, and operational stability across biological interfaces.

Keywords: hydrogels; iontronics; ion transport; wearable devices; bioelectronic interfaces

1. Introduction

Recent advances in flexible electronics, wearable devices, biointerfaces, and soft robotics have shifted sensing from rigid device integration toward dynamic coupling with biological tissues and complex fluids [1–3]. Accordingly, sensing materials must generate stable and readable signals in humid, saline, and biofluid-rich environments while maintaining long-term mechanical compatibility with soft tissues such as skin and organs [4,5]. Although electronic conductors, including metals, carbon-based materials, and intrinsically conducting polymers, are widely used in conventional electronics [6,7], their high modulus, poor interfacial matching, weak wet adhesion, and potential electrochemical side reactions limit their suitability for next-generation sensing systems requiring conformal, minimally invasive, and durable biointerfaces. To address these challenges, iontronics offers

a new paradigm in materials and device design [8]. Unlike traditional conductors that rely on electron or hole transport, iontronic devices use ions as the main charge carriers [9,10]. They enable signal transduction and amplification through ionic migration in electrolytes and modulation of interfacial electric double layer (EDL). This mechanism makes iontronics inherently compatible with hydrated environments and bioelectrochemical interfaces [11]. Among ionic conductors, hydrogels are especially attractive because they combine softness, wetness, and ionic conductivity. Their three-dimensional polymer networks provide stretchability, compressibility, self-healing, and adhesion [12–14], while their high water content forms continuous ionic pathways that support tissue-like conduction and diffusion. The hydrogels can be processed via solution casting, in situ polymerization, three-dimensional (3D) printing, or patterning, allowing fabrication of flexible devices that conform closely to skin and organ surfaces [15–17]. As a result, hydrogel-based iontronic sensing systems have shown broad potential in wearable pressure and strain sensors, electronic skin, bioelectrical signal monitoring, soft robotic haptics, environmental sensing, and healthcare interfaces [18–20].

Notably, HBIS is not merely about enhancing hydrogel conductivity. Its performance is fundamentally governed by ion transport mechanisms and electrochemical interfacial coupling. Ion movement within hydrogels is primarily driven by diffusion and electromigration. However, additional transport modes-such as convection, electroosmotic flow, and ion adsorption/desorption or site hopping mediated by ion-polymer interactions-can be triggered by mechanical deformation, concentration gradients, or external fields [21,22]. In proton-conductive or hydrogen-bond-network-rich matrices, a Grotthuss-type mechanism may also contribute to proton transport. Meanwhile, the EDL formed at the hydrogel/electrode or hydrogel/skin interface significantly influences device sensitivity, bandwidth, noise, and hysteresis [23]. In other words, the amplitude, response speed, and stability of sensing signals depend on a multiscale structure-transport-interface-circuit chain. Accordingly, the amplitude, response speed, and operational stability of HBIS are governed by a multiscale chain spanning structure, transport, interface, and circuit. At the microscopic scale, parameters such as network porosity, hydration degree, fixed charge density, ion solvation, and phase separation dictate effective ion mobility and diffusion length [24,25]. At the mesoscopic scale, interfacial capacitance, ionic redistribution, and concentration polarization regulate frequency response and hysteresis behavior. At the macroscopic scale, overall device geometry, electrode architecture, and readout circuitry ultimately define the signal-to-noise ratio and operating window [26].

Despite notable progress in this field, several critical issues remain unresolved. First, although many studies emphasize enhancing mechanical toughness, stretchability, and room-temperature conductivity, there is a lack of systematic analysis on how ion transport, ionic dynamics, and electrochemical coupling affect key sensing parameters-such as sensitivity, response time, frequency bandwidth, drift, and repeatability [27,28]. Second, the materials landscape is highly diverse, spanning ion-conductive hydrogels, polyelectrolyte hydrogels, ionic liquids or ionogels, and nanocomposite hydrogels incorporating nanofillers [29]. Nevertheless, the absence of unified classification frameworks and standardized, benchmarkable evaluation protocols continues to impede rigorous cross-study comparison [30,31]. Third, key challenges, including EDL interfacial hysteresis, frequency-dependent ion diffusion, drift [32], and memory effects associated with transient ionic redistribution during operation, are often underestimated or neglected. As a result, predictive device modeling remains limited and engineering reliability is undermined.

This review offers a systematic, framework-oriented synthesis of hydrogel-based iontronic sensors through a multiscale structure-transport-function perspective (Figure 1). First, we examine strategies for constructing ion-conducting pathways and mechanical and electrical properties, leveraging the composition and microstructural characteristics of various hydrogel systems. Second, we analyze how diffusion, electromigration, electroosmotic flow, and EDL kinetics influence signal generation, focusing on ionic transport and electrochemical interface dynamics. Quantitative analysis is supported by PNP theory and electrochemical impedance modeling [33]. We then review key sensor architectures, including EDL-capacitive devices, impedance-based sensors, and electrolyte-gated transistors (EGTs) [34]. Finally, we identify key challenges such as environmental instability, ionic redistribution, drift, interfacial hysteresis, low-frequency noise, long-term biointerface compatibility, and issues in encapsulation and packaging, offering future research directions to address these limitations [35,36]. By consolidating these insights, we provide a roadmap for the rational design of next-generation hydrogel-based iontronic sensors, with applications in healthcare, robotics, and other emerging domains.

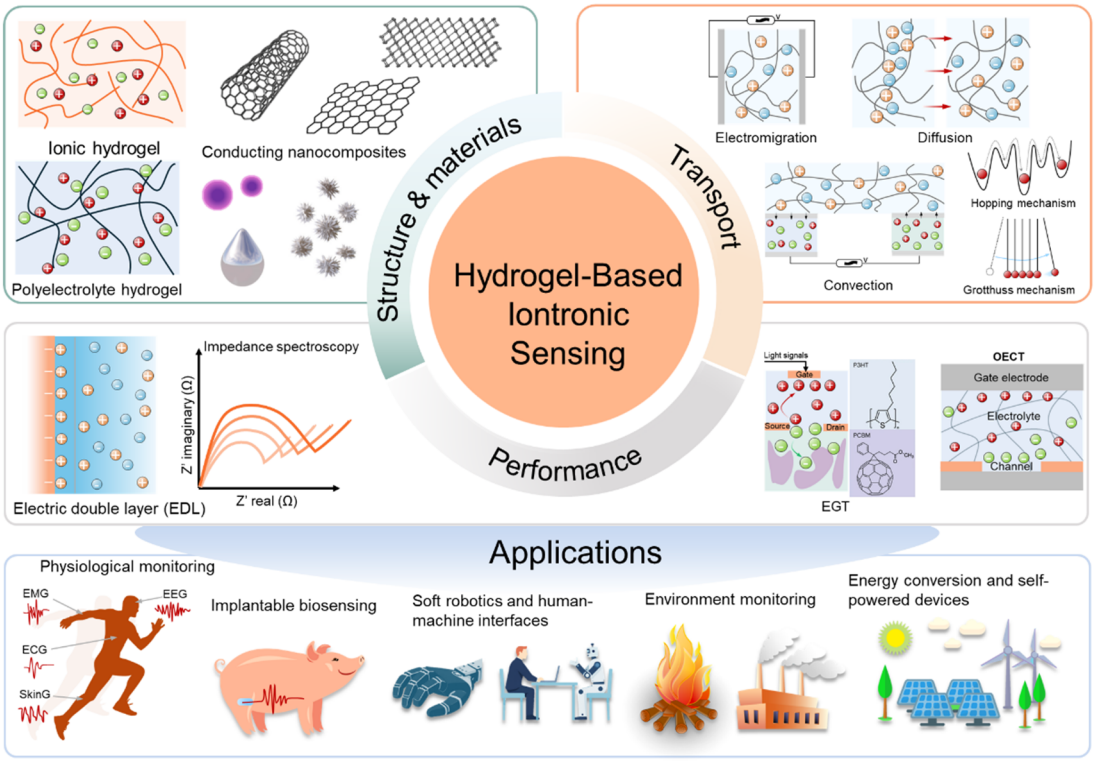

Figure 1. Brief outline of hydrogel-based iontronic sensing in this review.

2. Material Systems and Fundamental Models

2.1. Material Systems

2.1.1. Ion-Conductive Hydrogels and Polyelectrolyte Systems

Ion-conductive hydrogels (shown in Figure 2a) consist of three primary components: a three-dimensionally crosslinked polymer scaffold, a porous or channel-rich network, and mobile ions. Their conductivity arises from the directional transport of hydrated ions through interconnected pores, rather than from electronic carriers. Consequently, the incorporation of polyelectrolytes or additional salts directly determines the upper limit of ionic conductivity. Modern formulations commonly utilize acrylamide (AM), poly(vinyl alcohol) (PVA), or poly(acrylic acid) (PAA) to establish the initial polymer network, typically through free-radical polymerization or freeze-thaw physical crosslinking [37,38]. Mobile ions such as Na^+, Li^+, and Cl^- are then introduced to form continuous triphasic polymer-water-ion transport channels. These hydrogels benefit from mature fabrication techniques, are relatively cost-effective, and exhibit favorable biocompatibility [39,40]. These hydrogels can be readily processed into films or conformal structures, meeting the dual demands of adhesion and stretchability in wearable devices. In recent years, extensive research has focused on enhancing their overall performance. For instance, Hou et al. [41] reported an agar/NaCl/polyacrylamide (PAAm) double-network ionic hydrogel capable of monitoring biological motions such as joint bending, wrist pulse, and subtle throat muscle movements. In this system, conductivity, measured at approximately 0.04 $S \cdot m^{-1}$, was found to depend strongly on both salt concentration and network architecture.

On the other hand, increasing salt concentration or incorporating multi-network and coordination architectures can significantly enhance conductivity, reaching values around 0.7 $S \cdot m^{-1}$. For example, Zhang et al. [42] reported that doping 2 M NaCl into a PAAm/PAA-Fe^{3+} coordination network resulted in an ionic conductivity of approximately 0.72 $S \cdot m^{-1}$. Such materials have been applied in flexible strain and pressure sensors, as reviewed in the literature. However, traditional polymer hydrogels that rely solely on ion-filled channels often suffer from poor mechanical strength, limited toughness, and reduced fatigue resistance, which restrict their long-term functional stability. Meanwhile, factors such as ion hydration, polymer segmental motion, and dehydration can lead to long-term drift of ionic channels during operation, compromising electrical conductivity and sensing stability [19]. To overcome these limitations, Liza et al. [43] have created multinetwork/double-network (DN) and interpenetrating network (IPN) architectures, as well as hydration-solvent regulation and functional strategies such as anti-dehydration, anti-freezing, self-healing, and self-adhesion, to achieve a better balance between ionic conduction and long-term stability.

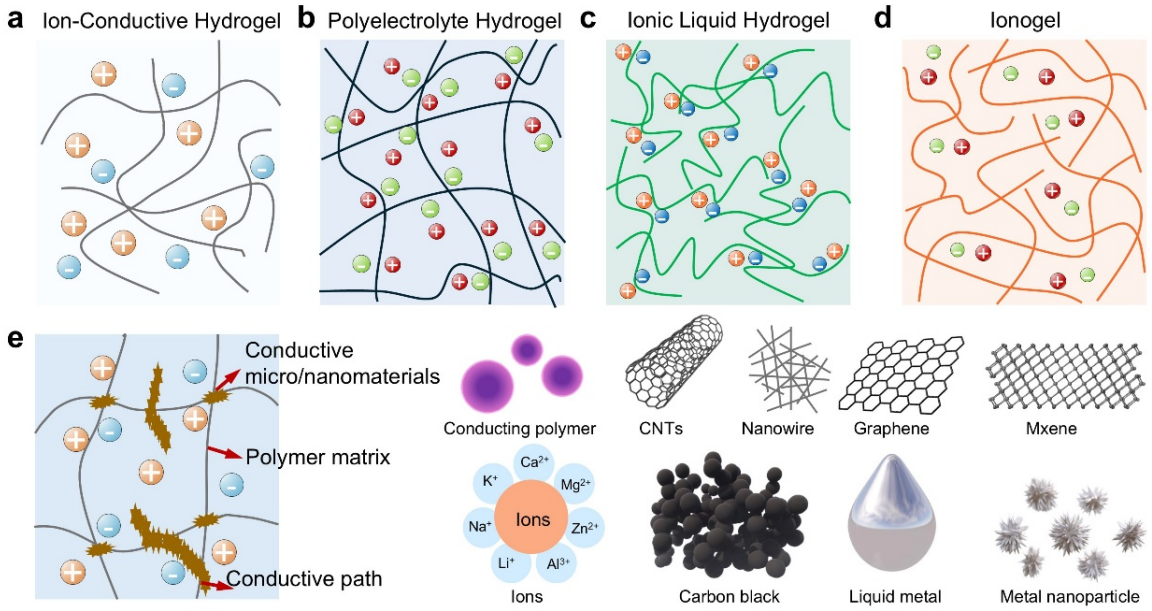

Figure 2. Conductive material components of HBIS. (**a**) Ion-conductive hydrogel. (**b**) Polyelectrolyte hydrogel. (**c**) Ionic liquid hydrogel. (**d**) Ionogel. (**e**) Conductive nanomaterials [44]. Copyright 2025, Elsevier.

Typical polyelectrolytes (shown in Figure 2b), such as PAA, sulfonated polystyrene (PSS), and perfluorosulfonic acid polymers (e.g., Nafion), possess covalently bound negative charges on their polymer backbone. In contrast, polymers like polyethylenimine (PEI), polyquaternary ammonium salts (e.g., poly(diallyldimethylammonium chloride) (PDADMAC)), and poly(4-vinylpyridine) (P4VP) carry positive charges. Unlike salt-doped ionic conductors, where free ions are dispersed in the matrix, the fixed charges in polyelectrolytes help minimize ion dissipation and leakage, thereby enhancing long-term signal stability in sensing applications [37,45]. However, ionic conduction and interfacial behavior in polyelectrolytes remain strongly influenced by fixed-charge density, segmental flexibility, and network topology. Fixed charges modulate counterion migration and diffusion, as well as the spatial extent and dynamic formation/relaxation of the interfacial electric EDL [28]. These factors collectively determine the polarization behavior and response speed of iontronic devices [46].

Recently, He et al. [47] reported a polyelectrolyte elastomer engineered through molecular structure design and copolymerization strategies to achieve both low creep and low ionic leakage. Iontronic sensors fabricated from this material exhibited significantly reduced signal drift and enhanced stability under sustained static pressure. This work highlights a design principle that improves signal fidelity by synergistically regulating fixed-charge density and mechanical relaxation behavior. Furthermore, Song et al. [48] integrated a low-creep polyelectrolyte into an iontronic wireless sensing system, enabling long-term, low-drift wireless readout for orthodontic load monitoring. This study underscores the critical role of material creep and ion leakage in influencing signal drift, highlighting their importance in the design of stable, high-fidelity sensing platforms.

Polyelectrolytes can also be processed into solid-state films or nanofibrous membranes for durable, wearable device applications [49,50]. For example, Wang et al. [51] developed a pressure sensor based on a polymeric ionic liquid (IL) nanofibrous membrane, fabricated by polymerizing an imidazolium-based ionic-liquid monomer (Figure 2c) followed by electrospinning. The sensor maintained stable performance after multiple water-washing cycles under high-humidity conditions, demonstrating that a design incorporating fixed charges and a fibrous network provides significant durability for wearable applications.

Notably, ionic conductivity in polyelectrolyte systems is often governed by the coupling between ionization/dissociation processes and polymer segmental motion. As a result, ambient humidity fluctuations can significantly influence both conductivity and interfacial polarization. While aqueous electrolytes typically offer higher ionic conductivity and faster ion transport kinetics, they suffer from a limited electrochemical stability window due to hydrogen and oxygen evolution reactions. Moreover, their performance is susceptible to water-content drift caused by evaporation or condensation. Consequently, sensing applications that prioritize long-term stability often require more rigorous co-design of materials and encapsulation strategies [52,53].

2.1.2. Ionic Liquid and Deep Eutectic Solvent Systems

Ionic liquid (IL) and deep eutectic solvent (DES) systems (Figure 2d) are often formulated as ionogels or eutectogels, in which IL/DES species are immobilized within polymer networks through chemical crosslinking, topological entanglement, or synergistic interactions with inorganic or nanoscale fillers [54,55]. These materials are stable across wide temperatures, providing consistent ionic conductivity under challenging conditions, ideal for flexible sensing and energy devices [56]. In recent iontronic and ionic-capacitive pressure sensing studies, Nie et al. [57] employed ionogels and ionic films as dielectric layers, exploiting the exceptionally large capacitance at ion-electron interfaces to achieve high areal capacitance and high sensitivity. This work demonstrates a representative strategy for achieving stable capacitive readout using IL-based ionogels. Additionally, Shi et al. [32] demonstrated humidity-insensitive ionogel arrays for pressure monitoring. Ionogels can be made via in situ polymerization or blending IL/DES with thermoplastics, with trade-offs between conductivity and mechanical stability.

Ionogels are typically fabricated using two main approaches: (i) in situ polymerization of IL/DES with crosslinkable monomers such as polyethylene glycol diacrylate (PEGDA) or hydroxyethyl methacrylate to form a polymer network; and (ii) blending and curing IL/DES with highly polar thermoplastic polymers. Their overall properties are primarily governed by the interplay among ionic-phase fraction, viscosity/mobility, and network mechanics. Increasing IL/DES content generally enhances ion transport but may compromise mechanical integrity by inducing softening and creep [26,31,58].

Moreover, due to the inherently high viscosity and limited ionic mobility of ILs, ionogels often exhibit lower ionic conductivity than hydrogels, necessitating trade-offs between conductivity and mechanical stability. These limitations can be mitigated by incorporating inorganic fillers and/or adopting multi-network architectures to fine-tune both ionic and mechanical performance [59]. DES systems are often employed as eutectogels to enhance anti-freezing and anti-drying performance, thereby expanding operational temperature ranges [60,61]. For instance, Hu et al. [62] demonstrated that a choline chloride (ChCl):urea-based DES gel maintained stable sensing performance even at low temperatures (−20 °C). Additionally, eutectogels formulated with hydrophobic DES can substantially mitigate performance drift caused by water uptake in humid environments. Nonetheless, IL/DES-based materials still face several challenges, including potential toxicity and biocompatibility concerns, high cost, limited miscibility or compatibility with polymer matrices, narrow processing windows, and risks of leakage or structural instability under continuous operation [56].

2.1.3. Nanofillers and Composite Reinforcement Strategies

To simultaneously enhance mechanical strength, toughness, cyclic fatigue resistance, and long-term stability of conductive networks, nanofillers such as carbon nanotubes (CNTs), graphene or MXene sheets, liquid metals and metallic/inorganic nanoparticles are increasingly incorporated to form nanocomposite hydrogels (as depicted in Figure 2e) [63,64]. These systems make use of an elastic matrix coupled with a rigid structure, wherein the nanofillers provide mechanical reinforcement, while the polymer network maintains flexibility and stretchability. This approach effectively reduces the conductivity-stretchability trade-off and improves signal fidelity and durability under complex deformation conditions. The shape, dispersion quality, and interfacial compatibility of nanofillers remain critical parameters in optimizing overall performance. Recently, Ren et al. [65] showed CNT-enhanced hydrogels improving conductivity and stretchability for strain sensing, while Hauck et al. [66] demonstrated graphene-based hydrogels improving water and ion transport. MXenes and carbon-based materials are crucial for high-performance hydrogel sensors [67].

From a device perspective, the electrode is a critical component of HBIS, as both electrical conductivity and interfacial impedance directly affect signal-transfer kinetics and long-term stability. Flexible electrodes typically consist of a flexible substrate and conductive phase configuration. Common substrates include polyimide, polydimethylsiloxane, and thermoplastic polyurethane [68,69]. The conductive phase may be composed of composite hydrogel. The composite components can encompass a wide range of materials, including conducting polymers, carbon-based materials, ions, ionic liquids, metallic materials, and liquid metals [64,70]. Carbon materials and conducting polymers offer good flexibility and processability but often require trade-offs in conductivity and environmental stability. A key trend is combining electronic and ionic conductors to reduce skin-contact impedance. For example, Li et al. [71] developed a poly(3,4-ethylenedioxythiophene): polystyrene sulfonate (PEDOT:PSS)-MXene composite hydrogel with high conductivity and low interfacial impedance, suitable for surface electrophysiological sensing. Overall, electrode material design must balance conductivity, flexibility, durability, interfacial impedance and fabrication cost [72].

The comparative table (Table 1) presented in this section provides a comprehensive overview of key performance metrics for various material systems, including ion-conductive hydrogels, polyelectrolyte hydrogels,

ionic liquid hydrogels, ionogels, and conductive nanomaterials. These metrics include ionic conductivity, mechanical properties, sensitivity, and stability, with specific references for each material. By summarizing these characteristics, the table allows for a direct comparison of the strengths and limitations of each material system. It highlights the diverse range of properties, such as high strain sensitivity in ion-conductive hydrogels, long-term stability in polyelectrolyte hydrogels, and excellent mechanical robustness in ionogels. Additionally, the table emphasizes the versatility of conductive nanomaterials in applications requiring high conductivity and flexibility. This quantitative summary significantly enhances the practical value of the section, providing readers with clear insights into the suitability of each material for iontronic sensor applications.

Table 1. Representative hydrogel-based iontronic material systems: conductivity, mechanical properties, sensing performance, and stability.

Material System	Conductivity	Mechanical Properties	Sensitivity	Stability	Ref.
Ion-conductive hydrogel	≈0.04 $S \cdot m^{-1}$	high toughness	High strain sensitivity	Biocompatible	[41]
	≈0.72 $S \cdot m^{-1}$	Enhanced toughness	Good strain/pressure	Improved long-term via multi-network	[42]
	\	Balanced toughness	Good strain/pressure	Anti-dehydration, self-healing, long-term stable	[43]
Polyelectrolyte hydrogel	\	Low creep	Reduced signal drift	long-term stability	[47]
	\	Low creep	Wireless load monitoring	Long-term low-drift	[48]
Ionic liquid hydrogel	\	Durable fibrous network	Stable capacitive pressure	Washable, moisture-proof	[51]
Ionogel	Lower than hydrogels	\	high sensitivity	Stable EDL response	[57]
	\	Mechanically robust	Intra-articular pressure	Humidity-insensitive, low-drift	[32]
	\	\	Stable pressure/temperature	Anti-freezing (−20 °C)	[62]
Conductive nanomaterials	Up to 2.3 $S \cdot m^{-1}$	Balanced stretchability	Strain sensing	Improved fidelity under deformation	[65]
	\	Flexible	Enhanced actuation	Improved ion/water transport	[66]
	High conductivity	Flexible	Electrophysiological sensing	Low interfacial impedance	[71]

The above material classifications not only differ in composition and structure, but also tend to exhibit different dominant ion-transport characteristics. In general, ion-conductive hydrogels mainly rely on diffusion and electromigration of hydrated ions within interconnected aqueous channels. Polyelectrolyte hydrogels, owing to their fixed-charge groups, more strongly involve ion-selective partitioning, interfacial redistribution, and electro-osmotic effects. Ionic liquid hydrogels and ionogels are likewise governed primarily by diffusion and electromigration, although ion association, viscosity, and non-aqueous solvation can substantially modify transport efficiency and interfacial dynamics. In nanocomposite hydrogels, transport becomes more heterogeneous because filler-polymer interfaces, adsorption/desorption, and tortuous pathways may contribute to site-assisted or hopping-like ion motion. Meanwhile, Grotthuss-type transport is more likely to be relevant in proton-conducting or hydrogen-bond-rich systems, rather than being universally dominant across all hydrogel classes. Therefore, the mechanisms discussed in the following section should be understood in the context of specific material systems, which together determine the final sensing behavior of HBIS.

2.2. Structure-Transport-Performance Relationships and Modeling

Material composition alone does not fully account for the high performance of HBIS. Ion transport behavior is strongly modulated by the microstructural features of the hydrogel network-such as topology, porosity, and phase separation as well as by solvation and hydration states and the spatial distribution of ions. These factors collectively play a pivotal role in determining key performance metrics including sensitivity, response speed, hysteresis, and long-term operational stability [69]. To establish quantitative correlations between structure and function, it is crucial to integrate detailed structural characterization with transport modeling. This enables the

development of clear structure-transport-performance relationships [12]. Building on this framework, we now examine how specific microstructural parameters govern the functional behavior of HBIS.

2.2.1. Network Structure, Porosity, and Phase Separation

The topology of hydrogels, which are made up of three-dimensionally crosslinked polymer networks, directly controls important structural characteristics. This topology is determined by factors like crosslink density, segment length, crosslinking process, and the existence of interpenetrating or double-network structures. These include segmental mobility, water content and swelling behavior, porosity, pore-size distribution, and the hydrogel's ability to hold and contain solvents or ions [69]. The effective paths and resistances for ionic transport within the matrix are defined by these characteristics taken together. Monomer-to-crosslinker ratios, initiation and polymerization settings, polymerization sequencing (e.g., one-step vs. stepwise), and techniques like double-network formation can all be used to customize the network design. By altering the microstructure, these techniques allow for exact control over ion transport characteristics [12]. Ionic and water distributions within hydrogels are highly sensitive to pore architecture and phase separation. Excessively large pores can lead to water loss and instability in conductive channels, while overly small pores may overly confine hydrated ions, impeding their mobility and reducing transport efficiency. Additionally, phase separation between polymer-rich and solvent-rich domains can result in the formation of distinct conductive regions, introducing heterogeneity in ion transport pathways. This structural irregularity may manifest as signal hysteresis, drift, and diminished frequency responsiveness. Accordingly, quantitative characterization of porosity and phase separation typically relies on scanning electron microscopy (SEM), X-ray/small-angle X-ray scattering (SAXS), freeze-dried morphology analysis, and measurements of water content/water retention, which, when combined with ion-transport models (e.g., Nernst-Planck, Donnan/Manning, solution-diffusion, and tortuosity models), can be used to back-calculate diffusion/migration parameters and their structural origins [73].

A recent research direction in this field focuses on multiscale porosity regulation and the creation of channeled ionic pathways. For instance, Dai et al. [74] demonstrated that microfluidic bubble-templating-assisted 3D printing can be used to fabricate ordered macroporous structures, enabling synergistic control over both the macroscopic geometry and internal porosity of hydrogel-based systems. In the domain of ionogels, Yang et al. [75] employed microbubble templating to develop a highly porous ionogel tailored for high-sensitivity, wide-range pressure sensing. Their work showed that engineered porosity significantly enhances EDL responsiveness and broadens the compressive deformation window, offering a practical strategy for next-generation flexible sensors.

In the meantime, different crosslinking techniques are strongly associated with different dynamic mechanical and sensory properties. Physically crosslinked systems, like the freeze-thaw PVA hydrogel described by Adelnia et al. [76], for example, often show significant viscoelastic dissipation and signal hysteresis. On the other hand, systems that use anti-dehydration techniques or chemically crosslinked networks can significantly improve signal repeatability and cycling consistency under repeated loading situations. Hydrogel dehydration continues to be a significant cause of performance loss at the device level, especially during extended operation. Ionogels, which have low volatility, or hygroscopic additives like glycerol, which retain interior moisture and maintain functional stability, can help with this problem.

In the future, a better mechanistic knowledge of structure-property connections is anticipated to be made possible by the ongoing development of sophisticated fabrication and characterisation techniques. The logical design of next-generation hydrogel systems will be guided by these findings, which will ultimately result in significant advancements in sensor performance, durability, and application scope.

2.2.2. Solvation Effects and Ion Distribution

A The internal environment of a hydrogel is not a uniform mixture of polymer chains, salt, and water. Rather, through hydrogen bonding, ion-polymer coordination, and electrostatic interactions, water molecules dynamically create solvation and hydration shells around both ions and polymer segments. The structure and rearrangement kinetics of hydration shells directly influence effective ionic mobility, diffusion coefficients, and the system's responsiveness to external stimuli such as electric fields, mechanical deformation, and fluctuations in temperature or humidity [77,78].

The concentration and spatial distribution of free ions can be greatly influenced by ion-ion correlations, such as ion pairing and clustering, as well as ion-polymer interactions, in high-salt environments or matrices containing ionic liquids or deep eutectic solvents. The population of conduction-active charge carriers is frequently reduced by these interactions, which causes a difference between the actual effective ionic flow and the observed bulk ionic conductivity. This mismatch can affect frequency-dependent responses and change the properties of signal

propagation, making it difficult to accurately interpret and maintain the stability of iontronic sensing signals [79]. Conversely, by optimizing the solvation environment and network chemistry, for example, boosting local polarity that promotes solvation and lowering unfavorable ion correlations, one can increase ionic freedom and response speed while retaining a high ion concentration. This can improve the integrated sensing performance of the material system [80].

Accordingly, establishing clear links among solvation structure, ionic distribution, and transport parameters is essential for understanding and optimizing iontronic performance. Molecular dynamics (MD) simulations and statistical thermodynamics models are valuable tools for capturing ion-ion correlations, local dielectric environments, and dynamic solvation behavior. These approaches offer atomistic insights into how ionic mobility is influenced by structural fluctuations and intermolecular interactions. Experimentally, a combination of spectroscopic and diffusion techniques is commonly employed. Nuclear magnetic resonance (NMR), infrared spectroscopy, and Raman spectroscopy help characterize solvation structures and ion-polymer interactions. In particular, pulsed-field-gradient NMR (PFG-NMR) enables direct measurement of self-diffusion coefficients for both water molecules and ions, offering a quantitative view of hydration effects on ionic migration [81].

Using PFG-NMR, Moon et al. [77] examined the self-diffusion behavior of ions and water in functionalized hydrogel membranes, showing that diffusivities are mostly controlled by the hydration state of the system. This discovery emphasizes how important water-ion interactions are for mediating transport in hydrated, soft networks. Concurrently, researchers in ionogels have investigated the interaction between ionic transport and polymer segmental dynamics, demonstrating the intricate and non-linear link between chain relaxation, ion correlations, and ionic conductivity [82]. These observations cast doubt on the notion of a simple structure-property mapping and imply that cooperative dynamics need to be taken into account when creating iontronic materials. Moving forward, improvements in simulation models and computer capabilities are likely to improve mechanistic analysis of how ion migration impacts conductive and sensing performance.

2.2.3. Modified PNP Modeling and EIS Parameter Extraction

At the macroscopic scale, ionic transport is often characterized by a unified diffusion and electromigration image, with the PNP model serving as the classical continuum framework. The Poisson equation represents the electric potential distribution caused by space charge, whereas the Nernst-Planck equation describes ionic fluxes and concentration evolution that is controlled by both concentration gradients and electric fields. Consequently, the PNP model allows for quantitative investigation of ionic distributions, electric-field responses, the creation of EDLs, and the associated current/conductance and impedance-frequency-dependent properties [33].

Hydrogels are not free liquid electrolytes, and therefore direct application of the classical PNP model is often insufficient. The polymer network introduces geometric confinement, pore tortuosity, local viscosity effects, delayed ion/solvent rearrangement, and in some cases fixed charges, interfacial adsorption/desorption, and hysteresis. Consequently, practical modeling often extends PNP by incorporating effective diffusion/tortuosity corrections, fixed-charge and Donnan terms, and interfacial boundary conditions such as surface charge and Stern layers, so as to better capture transport in gel networks and at electrode interfaces [83].

The combination of PNP modeling with electrochemical impedance spectroscopy (EIS) is particularly useful for hydrogel-based ionic devices. By applying small-signal AC perturbation and linearized analysis, frequency-dependent impedance can be predicted and fitted to Nyquist/Bode spectra, enabling extraction of key parameters such as diffusion coefficient, Debye length, and interfacial capacitance/resistance [84,85]. For instance, Balakrishnan et al. [33] presented a representative case in which PNP modeling was applied to the impedance spectra of NaCl-containing ionic conductors and used to evaluate strain and temperature sensing behavior, demonstrating the feasibility of model-EIS-device-performance approach.

In addition, PNP modeling is commonly used to analyze and design interfacial effects in hydrogel iontronic devices, such as EDL modulation and ionic rectification. Ouyang et al. [86] investigated ionic rectification induced by hydrogel interfacial EDL regulation, further illustrating how continuum modeling can support the interpretation and design of interface-dominated iontronic functions.

2.2.4. Multiscale Simulation and Statistical Modeling

Hydrogel-based iontronic systems typically involve multiple coupled processes, such as polymer networks, solvents/ions, fillers, and interfacial electric double layers; relying solely on macroscopic PNP models or equivalent-circuit/impedance descriptions is often insufficient to explain non-ideal behaviors caused by ion correlations, solvation rearrangements, network constraints, and interfacial adsorption. As a result, multiscale

modeling from the molecular to the device level, along with statistical physics approaches, is critical for establishing a quantitative relationship between microstructure, ion transport, and device response [87].

At the microscopic level, MD and coarse-grained molecular dynamics (CGMD) simulations can resolve ion-water-polymer interactions, ionic diffusion trajectories, and polymer segmental dynamics. Transport coefficients such as diffusion and conductivity can be extracted via Green-Kubo linear-response formalisms or mean-squared-displacement analyses. These approaches have matured into theoretical and modeling frameworks for ionic polymers and gel electrolytes [88]. At the mesoscale, modeling approaches such as Monte Carlo simulations, random-walk algorithms, phase-field methods, and porous-media or tortuosity-based models are commonly employed to reconstruct channelized transport pathways and spatial heterogeneity within hydrogel or ionogel matrices. These models enable the upscaling of microscopic transport characteristics, such as ion mobility and local diffusivity, into macroscopic effective diffusion and migration behaviors, bridging the gap between structure and function in complex, heterogeneous materials [89].

Diffusion coefficients (D), ion mobilities (μ), and interfacial boundary conditions (such as surface charge density, adsorption/desorption kinetics, and the presence of Stern layers) are examples of microscopically derived parameters that are typically integrated into continuum-scale models at the device level. These models, which are frequently based on the PNP or related electrokinetic frameworks, allow the simulation of interfacial dynamics, charge transport, and field distribution across intricate device geometries, connecting macroscopic sensor behavior with molecular-scale events. These models are then jointly fitted with EIS, frequency-response, and transient-response data to enable parameter inversion and structural optimization [56,90]. For example, Lu et al. [82] reported on ionogels and have combined macroscopic mechanics/conductivity measurements with EIS and microscopic characterization of chain and ionic dynamics to directly reveal the coupling between segmental dynamics, ion transport, and mechanical creep as ion content varies, providing a foundation for predicting device stability from material formulations. Another representative example of effective simulation-experiment coupling was reported by Ouyang et al. [91], who designed geometrically asymmetric polyacrylamide hydrogel iontronics for mechano-driven neuromimetic logic gates. In this work, COMSOL Multiphysics simulations of Darcy fluid velocity were integrated with ANSYS finite-element analysis of stress-strain distributions to reveal how thickness asymmetry induces localized stress concentration and thereby enhances ion convection within the hydrogel. The simulated results were consistent with the experimentally observed amplification of piezoionic output, directly demonstrating that structural asymmetry can be used to predictably regulate mechano-fluid-ionic coupling and sensing performance. This example is particularly valuable because it shows that multiscale simulation can do more than describe transport processes; it can also explain why a given structural design improves signal output and provide a rational basis for optimizing self-powered iontronic devices.

Thus, transferring experimentally accessible performance criteria onto a succinct collection of transferable and fit-ready parameters should be the main goal of modeling hydrogel-based iontronic sensors. Ion mobility, effective diffusivity, bulk conductivity, elastic modulus, interfacial EDL capacitance [80], and signs of hysteresis or signal drift are some of these. These models should be jointly constrained by a consistent experimental toolbox, specifically EIS, frequency-domain analysis, and cyclic mechanical loading, to enable predictive rather than purely empirical design. This will guarantee quantitative alignment between modeled behavior and real-world device performance [92].

2.2.5. Mechanism-to-Parameter Mapping

The review provides a four-dimensional mapping framework to direct the experimental design and optimization of HBIS. The framework systematically links experimental procedures, observed performance metrics, governing physical parameters, and underlying transport mechanisms, thereby enabling a coherent interpretation of structure-property-function relationships (Table 2). It works well with coupled mechanisms in complicated systems. It provides a detailed roadmap for cross-scale optimization across molecules, structures, and devices. The framework allows for the faster development of high-performance and high-stability HBIS. It can also accelerate translation to applications including wearable monitoring, implantable sensors, and human-machine interaction.

Table 2. Mechanism-to-parameter mapping for hydrogel-based iontronic sensing.

Mechanisms	Observable Signatures	Key Parameters	Performance Aspects Impacted	Experimental Design
Diffusion (PNP)	Warburg-type low-frequency dispersion (45° line in Nyquist)	Effective diffusivity D_{eff}, diffusion length L	Sets recovery time, low-frequency drift,	Scan L (thickness/electrode spacing): $\tau \propto L^2$ indicates diffusion control
Electromigration (PNP)	Faster transient current under higher field	Mobility μ, free-ion concentration c, field $E = -\nabla\varphi$	Controls response speed and nonlinearity	Small-signal vs. large-signal comparison
Convection (deformation-driven)	Spike-like fast component plus slow relaxation	Pore-fluid velocity v (or Darcy permeability k), solvent content	High-frequency response, repeatability at low frequency	Control pore structure/permeability
Electroosmotic flow (EOF)	Frequency-asymmetric and load/unload-asymmetric response	Debye length λ_D, ζ-potential	Drives asymmetry, rectification, and drift via ion-solvent coupled transport	Quantify asymmetry/rectification vs. λ_D to attribute to EOF/EDL overlap
Site hopping	Temperature-dependent kinetics	Activation energy E_a, distributed time constants	Contributes to hysteresis, drift, and frequency dispersion	Modulate surface/functional group density to test whether drift
Grotthuss-type	Strong dependence on hydration/H-bond integrity	Effective mobility μ_{eff}	Boosts high-frequency bandwidth and fast response	Tune H-bond network
EDL	Large capacitance changes with small contact-area/ion-distribution changes	Debye length λ_D, double-layer capacitance C_{dl}	Core origin of high sensitivity; governs bandwidth-hysteresis trade-off	Microstructure/contact-area control
Active gating (EGTs/OECTs)	EDL-gated or electrochemical-gated	Channel conductivity change $\Delta\sigma_{ch}$, gate-voltage window	Enables sensing-computing integration; impacts hysteresis and stability	Pulse-gating transient/steady tests, evaluate ionogel gating for stability

3. Ion Transport Mechanisms and Signal Transduction

3.1. Ion Transport Mechanisms

The signal origin of HBIS is not a single process, but rather the combination of several ion-transport mechanisms that occur in the bulk phase and in the EDL at the electrode-hydrogel interface. In a continuous description, the ionic flux can be calculated as the total of diffusion, electromigration, and convection. Additional mechanisms may emerge as a result of the combined effects of porous networks, fixed charges, and interfacial electric fields, such as electroosmotic flow (EOF), effective flux redistribution induced by interfacial adsorption/desorption, and Grotthuss-type hopping conduction in protonic or hydrogen systems [93,94]. These mechanisms correspond to various device readout modes (e.g., impedance-based, EDL-capacitive, EGTs/organic electrochemical transistors (OECTs)), and collectively (as depicted in Figure 3) determine the physical origins of response speed, frequency bandwidth, linearity, hysteresis, and drift, with diffusion and electromigration serving as the PNP framework's core backbone [19].

Unlike conventional electronic conductors, hydrogel charge carriers are primarily mobile ions like Na^+, Li^+, H^+, and Cl^-. Their electrical activity is affected by solvation/hydration shells, ion-polymer interactions, and interfacial activities. As a result, macroscopic conductivity may not correlate to effective ionic flow or interfacial signal amplification capabilities. Using ionic-capacitive pressure sensing as an example, the formation and modulation of the EDL are critical for achieving high sensitivity, and related reviews and device demonstrations have systematically summarized the relationship between EDL capacitance, ionic migration, and frequency response [46].

With respect to particular transport modes, proton and hydroxide conduction can occur via coupled vehicular and Grotthuss mechanisms. Zhang et al. [95] reported cooperative vehicular-Grotthuss OH^- transport in a double-network hydrogel, which explains its exceptionally high ionic conductivity and transport effectiveness. In contrast, EOF and ion-solvent coupled transport in narrow pores are frequently overlooked in iontronic devices, despite their potential impact on dynamic behavior, and Colla et al. [96] emphasized that elucidating EOF in nanopores and porous channels remains a central challenge for ionic-system modeling.

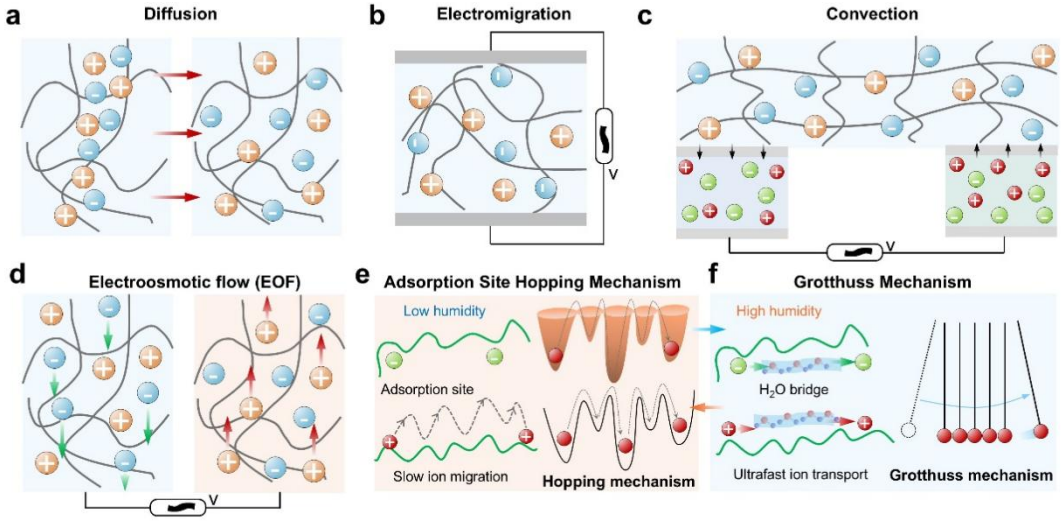

Figure 3. Schematic illustrations of ion transport mechanisms of HBIS. (**a**) Diffusion. (**b**) Electromigration. (**c**) Convection. (**d**) EOF. (**e**) Adsorption Site Hopping Mechanism. (**f**) Grotthuss Mechanism.

3.1.1. Diffusion

The most fundamental and common ion-transport mechanism in hydrogels is diffusion (Figure 3a), which is the spontaneous migration of ions driven by concentration gradients. Fick's law describes it ($J_i = -D_{eff}\nabla c_i$). Diffusion rates in hydrogels are influenced not only by intrinsic ion size and solvent viscosity, but also by network porosity/tortuosity and solvation state, and are thus frequently described as an effective diffusion coefficient [77,97,98].

In iontronic sensing, diffusion determines a critical characteristic timeframe ($\tau \sim L^2 / D_{eff}$), where L represents an effective diffusion length, such as gel thickness, pore connectivity length, or electrode spacing. For example, slower diffusion rates lead to delayed ionic redistribution following mechanical deformation or polarization, resulting in slower recovery times and increased baseline drift. This is particularly critical in systems requiring fast recovery, as diffusion-limited transport can extend the time required for the sensor to return to baseline after deformation or electrical stimulation. Additionally, during quick deformation or high-frequency stimulation, diffusion-limited transport can cause frequency-dependent response delays, leading to reduced sensitivity in high-frequency applications. These effects are particularly relevant in dynamic sensing applications, where the speed of ion transport plays a crucial role in the device's ability to capture rapid changes. Small-signal AC perturbation modeling within the PNP framework has directly shown how diffusion-potential coupling influences the impedance spectra and frequency-dependent sensitivity of ionic strain and temperature sensors. These findings provide a method for inverting D_{eff} and associated length scales using electrochemical impedance spectroscopy [33,99].

From an experimental standpoint, diffusion often manifests in electrochemical impedance spectroscopy (EIS) Nyquist/Bode spectra as Warburg-type diffusion impedance or low-frequency dispersive capacitance, typically shown by the characteristic 45° line and phase delay, with extensions to finite-length diffusion regimes. The theoretical derivation and equivalent-circuit formulation of diffusion impedance have been thoroughly explored in electrochemical impedance theory and adapted for nanoporous and porous media to provide more physically accurate descriptions.

3.1.2. Electromigration

Electromigration (Figure 3b) is one of the key mechanisms influencing hydrogels' direct current (DC) conductivity and transient current responsiveness. Within a continuum description, the electromigration flux is determined by ionic charge number, mobility, and the local electric-potential gradient, and together with diffusion constitutes the core transport basis of ion migration in hydrogel systems [33].

In hydrogels, electromigration is influenced by several factors, including effective ionic charge, solvation drag, pore tortuosity, and ion–polymer interactions such as hydrogen bonding and electrostatic adsorption/coordination. These factors directly affect ion mobility and field-driven redistribution, and thereby influence response speed, bandwidth, and signal nonlinearity. Electromigration directly controls response speed and nonlinearity through the key parameters of ion mobility μ, free-ion concentration c, field E=-φ. Under an applied voltage, enhanced electromigration accelerates counterion accumulation at the hydrogel–electrode interface, resulting in rapid EDL charging. This leads to shorter response times, higher bandwidth, and improved

sensitivity. As a result, under identical voltage excitation, systems with higher ionic mobility or lower solvation-induced resistance often show faster interfacial EDL charging/discharging, stronger transient currents, and a higher bandwidth limit. However, too high electromigration can more easily cause concentration polarization and interfacial hysteresis, resulting in nonlinearity, hysteresis, and drift, which must be controlled by coordinated design of materials and interfacial structures [33].

As an example, He et al. [47] achieved significantly low drift in iontronic sensing by designing polyelectrolyte elastomers with low creep and low leakage, demonstrating a strategy in which fixed charges and controlled network relaxation suppress field-driven ionic redistribution and leakage, improving readout stability under electromigration. From a mechanistic perspective, this example highlights the importance of controlling electromigration-induced ion accumulation and leakage, while the detailed use of PNP/EIS as a quantitative extraction tool is discussed in Section 2.2.3 [33].

3.1.3. Convection

Convection (Figure 3c) refers to the contribution to ionic flux originating from bulk fluid motion that transports ions. In continuum models, it can be expressed as $J_{conv} = cv$, where v represents fluid velocity. This term is frequently ignored in hydrogel-based iontronic sensing. However, for highly hydrated and porous gels, compression, shear, stretching, or external fluid flow can induce Darcy-type seepage of pore water, which transports ions, superimposing additional current or potential variations and producing non-negligible mechano-fluid-ionic coupling signals [100]. Convection mainly controls repeatability at low frequencies and high-frequency responsiveness through the parameters of pore-fluid velocity v (or Darcy permeability k) and solvent content. When the hydrogel undergoes rapid compression, shear, or stretching, the induced Darcy-type seepage of pore water generates a sharp, spike-like current component, enabling significantly faster signal rise times and markedly enhanced high-frequency bandwidth. Convection is therefore very useful for picking up high-frequency vibrations, impacts, or dynamic mechanical stimuli.

This mechanism is especially important in two scenarios: (i) force-fluid coupled sensing, in which external forces cause brief pore-water migration and promote convective ion redistribution. For example, Biutty et al. [101] offered a mechanism in which pressure drives cation convection, leading to electrode capture, explaining the output of self-powered pressure sensors in terms of convective ionic fluxes. The second situation concerns fluid/environmental monitoring, when devices work within fluid boundary layers such as sweat or within microfluidic channels, external flow affects interfacial mass transfer and ion exchange, modifying EDL charging states and steady-state potentials. For example, Zhang et al. [102] reported hydrogel-based sweat chloride sensors use skin-mounted microfluidic structures to achieve self-driven sweat collection and steady readout, effectively incorporating external convection/flow into the device's operation. Airflow-induced surface moisture absorption/desorption can influence near-surface network density and ionic mobility, resulting in resistive responses and a convection-related readout paradigm in which flow causes humidity changes that impact ion transport [103].

From an experimental signal perspective, convection-dominated processes often exhibit a two-timescale characteristic consisting of a fast spike followed by prolonged relaxation. The initial spike results from a temporary charge imbalance caused by convective ion flux, whereas the longer recovery stage is regulated by diffusion-mediated replenishment and interfacial EDL recharging. Convective transport can increase the possible bandwidth in applications that need high-frequency vibration or impact detection. However, for low-frequency steady-state monitoring, convection and seepage can cause stochastic drifts. As a result, convective effects are frequently limited by reducing gel permeability and creep, enhancing encapsulation to isolate external flow disturbances, or using controlled microfluidic structures [100].

3.1.4. Electro-Osmotic Flow (EOF)

Electro-osmotic flow (Figure 3d) is a fundamental electrokinetic phenomenon in which net charges within the EDL adjacent to channel or porous-medium walls experience Coulomb forces and drag solvent molecules, resulting in bulk liquid flow relative to the solid surface. When compared to pressure-driven flow, EOF in microchannels often exhibits a quasi plug-like velocity profile, permitting more controlled and low-dispersion mass transport, and is thus commonly used for fluid manipulation and sample transport in microfluidic and bioanalytical systems [104].

In hydrogel/polyelectrolyte systems, the permeable network and the presence of fixed charges promote the creation of stable EDLs at interfaces, allowing for EOF. EOF primarily drives frequency-asymmetric and load/unload-asymmetric responses, as well as rectification and drift, through the key parameters of Debye length

λ_D and zeta potential ζ. When an external electric field is applied, EOF causes a directional flow of ions-carrying solvent, which either speeds up or slows down local ion redistribution and produces a noticeable asymmetry in the sensing signal under alternating fields or loading vs. unloading cycles. As a result, a single material can function as both an iontronic sensing medium and an ionic pump or microactuator, allowing for electrical-to-fluidic signal translation or the opposite mapping of flow disturbances to electrical outputs. As a result, EOF is frequently overestimated, but crucial in evaluating load-unload asymmetry or frequency-dependent drift near porous interfaces [96].

As a representative example, Wang et al. [105] integrated a hydrogel-based electro-osmotic pump with Parylene C-coated porous microneedles, achieving enhanced EOF by using paired anionic/cationic hydrogels to enable controllable molecular transport through transdermal pathways. Although the application focuses on medication delivery, the physical mechanism is similar to iontronic sensing. It entails external-field manipulation of the EDL, generating EOF, and modifying local ion distribution and interfacial potential. This method is immediately applicable to sensing architectures for sweat flow, exudates, and shear-induced fluid changes. Another example is that Kusama et al. [106] reported a permeable microneedle array patch. In this study, sulfonated negatively charged hydrogels were inserted into microneedle channels to enhance transdermal EOF, demonstrating how fixed-charge density affects EOF flow rate and trans-barrier transport efficiency.

3.1.5. Adsorption Site Hopping Mechanism

When ions interact aggressively with polymer segments or filler surfaces, their transport changes. These interactions include electrostatic adsorption, coordination, hydrogen bonding, and ionic liquid-polymer contact. Under these conditions, ion transport no longer occurs via free diffusion or electromigration, as it does in the aqueous phase. Instead, ions move by thermally stimulated hopping. They move through a sequence of transitory bound states, sometimes known as adsorption sites hopping (shown in Figure 3e). Adsorption-site hopping often has higher energy barriers than the continuous, bridge-like fast transport of protons via the Grotthuss mechanism in hydrogen-bond networks, resulting in slower migration and transport characteristics dominated by hopping-relaxation processes [107].

At the macroscopic level, this mechanism is commonly associated with two observable effects. First, the dependence of conductivity on frequency or temperature more readily exhibits dispersion and non-simple Arrhenius behavior, which is governed by both site occupation-release dynamics and structural relaxation. Second, in certain structural designs, when adsorption sites create continuous pathways along surfaces or one-dimensional fillers, ions can flow directionally over a site network, which can help minimize drift and memory effects produced by random redistribution [108].

Through an ion-hopping migration mechanism, Zhu et al. [107] designed an oxygen-rich poly(urea–urethane) (OR-PUU) polyacrylamide-based hydrogel electrolyte that produces homogeneous zinc deposition in aqueous zinc-ion batteries. The carbonyl groups along the long-chain OR-PUU polymers typically hold partial negative charges due to dipole production, creating temporary intermediate states that aid Zn^{2+} hopping migration. These polymers also disrupt hydrogen bonding, accelerate ion transport, and promote Zn^{2+} desolvation, enhancing ionic conductivity while suppressing dendrite growth. This design supports fast ion transport and well-aligned Zn^{2+} deposition, offering a promising solution for wearable, dendrite-free zinc batteries. Moreover, Li et al. [109] reported a conductive PEDOT:PSS hydrogel with a hierarchically heterogeneous network topology. Densely packed PSS assemblies significantly lower the energy barrier for electron hopping between PEDOT microcrystallites in the hydrated state, enabling effective electronic transport. In comparison to ion-based processes, the charge transport velocity is around five orders of magnitude higher. Time-resolved electrochemical analysis of biological processes is made possible by the hydrogel's kinetically sensitive ion-electron transduction capacity.

3.1.6. Grotthuss Mechanism

The Grotthuss mechanism (Figure 3f) transports H^+/OH^- via bond breaking, reorientation, and relay processes. Effective charge migration does not require the vehicular motion of entire hydrated ion clusters, resulting in higher apparent mobility and faster electrochemical/impedance responses. For hydrogels in which protons or hydroxide ions dominate charge transport and have dense hydrogen-bond networks, such as highly hydrated matrices rich in -OH/-NH- groups or nanocellulose, the Grotthuss contribution frequently determines device response speed and bandwidth [110].

Notably, a hopping pathway does not have to be a macroscopically continuous aqueous phase; nanoscale confined water channels or interfacial water bridges can also form highly efficient proton-hopping pathways, causing conduction behavior to deviate from the simplistic the wetter, the more conductive paradigm.

Ichikawa et al. [111] verified surface proton hopping conduction, which involves protons quickly hopping between surface -SO_3^- sites via bridging water molecules. This highlights the amplification of hopping conduction via surfaces and nanoconfined channels.

In a double-network hydrogel (bacterial cellulose (BC)-polyacrylamide (PAM)-poly[3-(Methacryloylamino) propyl] trimethylammonium chloride (PMPTC)), Zhang et al. [95] found that OH^- conduction occurs by a synergistic combination of vehicular transport and the Grotthuss mechanism. The polymeric conductive framework provides continuous paths for hydrated-ion migration, while the hydrogen-bond network generated by bacterial cellulose adds additional hopping relays, significantly increasing OH^- conductivity. This type of synergistic mechanism implies that, without sacrificing mechanical strength, reinforcing hydrogen-bond networks can improve the response speed and frequency bandwidth of iontronic sensors, especially for high-frequency applications like tactile sensing and vibration detection.

Wang et al. [112] developed a Hofmeister-electrostatic ion-engineering strategy in which different Hofmeister anions direct the ordered assembly of Mo7 polyoxometalates with $Fe3^+$ to form a fully inorganic proton-conducting hydrogel. Charge inversion is induced by salting-in anions. They also promote the growth of one-dimensional supramolecules. This creates networks of coordinated, continuous hydrogen bonds. These networks allow proton transfer of the Grotthuss type. The activation energy consequently falls. Over a large temperature range, proton conductivity stays high. This facilitates thermal safety monitoring and accurate temperature detection.

Yang et al. [113] suggested controlling ion transport via a Janus-structure approach. An electrolyte with asymmetric hydrogen-bond networks and solvation environments was created by them. As a result, a cooperative Grotthuss-vehicle pathway is made possible for quick OH^- transport and extended device lifetime. Grotthuss hopping by hydrogen-bond rearrangement is preferred by one side, whereas vehicle-type carrier migration is promoted by the other. When combined, they reduce activation energy, boost ion mobility, and provide stable, effective alkaline ion conduction.

Before discussing the specific signal transduction pathways, it should be emphasized that the relationship among material systems, ion transport mechanisms, and electrical readout modes in HBIS is not strictly one-to-one, but is instead governed by predominant coupling between structure, transport, and interface. In general, conventional ion-conductive hydrogels and ionogels mainly rely on diffusion and electromigration through continuous ionic pathways, and therefore more often contribute to resistive or impedance-based transduction. Polyelectrolyte hydrogels, due to their fixed-charge groups and ion-selective environments, are more closely associated with interfacial ion redistribution, EDL regulation, and electro-osmotic effects, making them especially relevant for capacitive and interfacial signal transduction. In nanocomposite hydrogels, filler-polymer interfaces, heterogeneous pore structures, and adsorption/desorption processes can introduce more complex transport behaviors, including site-assisted transport and amplified interfacial polarization, which are often reflected in electrochemical or hybrid signal outputs. In addition, proton-conducting or hydrogen-bond-rich hydrogel systems may involve Grotthuss-type transport, which can become important in selected electrochemical and ion-modulated device architectures. Therefore, the four transduction pathways discussed below should be understood as functional manifestations of specific material-dependent transport processes, rather than as isolated electrical readout modes.

3.2. Transduction Pathway Electrical/Electrochemical Signal Transduction Pathways in HBIS

Although ionic migration itself is not directly observable, its electrical manifestations—such as changes in resistance, impedance, capacitance, current, and transconductance—form the critical link between ion transport and device performance in HBIS. Importantly, these signal transduction pathways do not arise independently of the material system, but instead reflect how different hydrogel structures regulate specific transport processes and interfacial responses. In general, resistive and impedance-type signals are most commonly associated with diffusion- and electromigration-dominated transport in ion-conductive hydrogels and ionogels; interfacial EDL modulation is more prominent in systems with strong interfacial charge regulation, such as polyelectrolyte and nanostructured hydrogels; electrochemical readout and modeling become especially important when adsorption, polarization, and heterogeneous ion transport strongly affect the device response; and active ion-modulated architectures, such as electrolyte-gated transistors (EGTs/OECTs), rely on controlled ionic coupling between hydrogel electrolytes and electronic channels. Therefore, this section discusses four representative transduction pathways—resistive/impedance responses, interfacial EDL modulation (Figure 4a), electrochemical characterization/modeling, and active ion-modulated architectures—in the context of their underlying transport origins and material dependence [46].

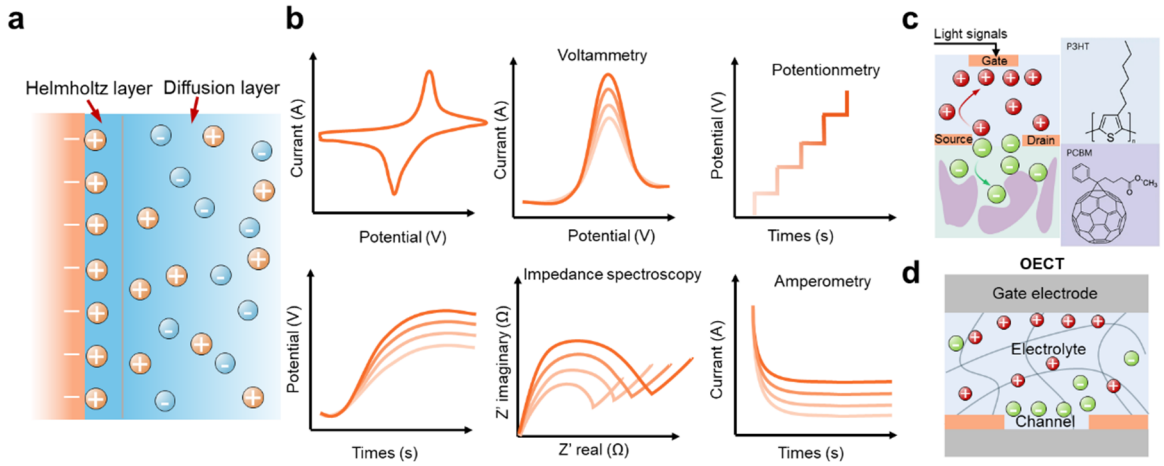

Figure 4. Schematic illustrations of the signal transduction pathways of HIBS. (**a**) Interfacial EDL modulation. (**b**) Signal transduction principles for HIBS. (**c**) Schematic representation of EGTs [114]. Copyright 2023, Springer Nature. (**d**) Schematic illustration depicting the gel-gated OECTs.

3.2.1. Electrical Resistance and Impedance

The direct-current resistance (R) of hydrogels might be considered a static indicator of macroscopic ionic transport: $R = \frac{L}{\sigma A}, where\ \sigma \propto \mu c.$ Here, L denotes the electrode spacing, A the effective cross-sectional area, and σ the ionic conductivity, which is jointly determined by the ionic mobility (μ) and effective charge-carrier concentration (c). Mechanical loading, such as stretching or compression, causes both geometric terms (L, A) and the transport term (σ) to change simultaneously. As a result, impedance-type responses often combine structural deformation with ion-transport modulation [33].

Compared to DC resistance, EIS can discriminate between bulk conduction, interfacial polarization/capacitance, and diffusion-limited processes. In practice, the Randles circuit is commonly used as a starting point, consisting of a solution/bulk resistance (R) in series with a parallel combination of interfacial capacitance (or constant phase element) and a Faradaic branch (e.g., charge-transfer resistance). When both kinetics and diffusion govern the system, a Warburg element can be introduced to represent diffusion impedance.

The frequency-domain characteristics of hydrogel-based ionic devices can be reduced to the following: Geometric/bulk resistance dominates high-frequency behavior, while interfacial polarization and diffusion-related contributions emerge at mid-to-low frequencies. Warburg impedance (semi-infinite or finite-length diffusion) appears as an approximately 45° line in Nyquist plots and manifests characteristic slopes and phase lags in Bode plots, allowing the extraction of diffusion coefficients and effective diffusion lengths [46,115]. This pathway is most commonly observed in ion-conductive hydrogels and ionogels, where diffusion and electromigration through continuous ionic channels dominate the signal generation process.

As a modeling case directly relevant to hydrogel-based iontronic sensing, Balakrishnan et al. [33] developed a PNP-based EIS theoretical framework and conducted experiments on NaCl ionic conductors to demonstrate how diffusion-potential coupling shapes impedance spectra, phase response, and frequency-dependent sensitivity, providing a reusable paradigm for quantitatively extracting transport parameters from EIS.

3.2.2. Electric Double Layer (EDL) Mechanism

The EDL is the most crucial interfacial amplifier in iontronic devices. When a hydrogel comes into contact with a metal electrode, biological tissue, or another electrolyte, interfacial fixed charges attract counterions, forming a compact Stern layer followed by an outer diffuse (Gouy-Chapman) layer, resulting in a nanoscale charge-separation structure with strong capacitive behavior. The Debye length (λ_D) describes the thickness of the EDL and is determined by ionic strength, ion valence, dielectric constant, and temperature. When the channel dimension approaches λ_D and EDL overlaps, interfacial phenomena including ion selectivity and rectification might emerge [57,116–118]. This pathway is particularly relevant to polyelectrolyte-rich or interfacially active hydrogel systems, in which fixed charges, ion-selective partitioning, and interfacial polarization strongly regulate signal output.

In iontronic sensing, the EDL capacitance is frequently approximated as $C_{dl} \approx \frac{\varepsilon_r \varepsilon_0 A}{d_{EDL}}$. Here, the symbol A represents the effective contact area, while $d_{EDL} \sim \lambda_D$ is measured in nanometers. Consequently, even modest changes in ion distributions or contact area can cause significant capacitance modulation, making this a highly sensitive signal source. The dynamics of EDL construction are determined by $\tau \approx R_{ion} C_{dl}$ (or, more broadly, distributed time constants), which determine the upper bounds of device bandwidth and hysteresis/drift [46].

Typical device paradigms mainly include: (i) Ionic-capacitive pressure/tactile sensing uses microstructures or compressible media to amplify contact-area fluctuations, resulting in ultrahigh specific capacitance and highly sensitive outputs, with the EDL serving as the primary mechanism [46]. (ii) EDL-modulated ionic rectification/switching: Asymmetric management of interfacial charges and EDL structures allows for rectifying and diode-like behavior, which can also be employed to reduce or explain frequency-dependent asymmetry and hysteresis [86]. (iii) Hydrogel-electrode interfacial energy/signal devices. Increasing EDL synergy at hydrogel-electrode interfaces improves directional ion migration and output stability, demonstrating the direct performance influence of interfacial EDL design [119].

The principal issues are focused on low-frequency noise, hysteresis, and drift, which are frequently caused by ion adsorption/desorption, interfacial water and dipole rearrangement, and non-ideal electrode surface characteristics. From an engineering standpoint, constant phase elements (CPE) and distribution of relaxation times (DRT) investigations are often used to define multitime-constant interfacial relaxation, allowing for quantitative connection of hysteresis/recovery processes to material and interfacial features [120].

3.2.3. Electrochemical Characterization and Modeling

Electrochemical characterization converts charge-transport and charge-storage activities at electrode/hydrogel interfaces and throughout the bulk phase into usable signals like current, potential, and impedance (as depicted in Figure 4b). The three-electrode system (working electrode (WE), reference electrode (RE), counter electrode (CE)) is a popular experimental arrangement. Interfacial processes can be isolated from bulk transport and characterized independently by accurately regulating the voltage between the WE and RE and monitoring the current in the WE-CE circuit [115,121]. In hydrogel-based iontronic devices, characterization often focuses on non-ideal processes such as diffusion and polarization, rather than analyte Faradaic reactions. This pathway becomes especially important in materials with heterogeneous interfaces or adsorption-active sites, such as nanocomposite hydrogels, where non-ideal transport and polarization behavior require electrochemical analysis for interpretation.

Consequently, EIS is particularly important: a small-amplitude sinusoidal perturbation is applied to a steady-state system while sweeping frequency to obtain the frequency-dependent complex impedance, which is then fitted with equivalent circuits to extract parameters such as R_Ω, C_{dl}/CPE, and diffusion-related Warburg elements [122]. In Nyquist plots, the high-frequency semicircle typically represents parallel interfacial charge-transfer resistance and capacitance, whereas the low-frequency linear segment represents diffusion limitation. These properties enable the delineation of bulk resistance, interfacial polarization, and diffusion control, as well as correlation with device bandwidth, hysteresis, and drift [123].

In recent years, more material-oriented standardized EIS measurement techniques and device designs have arisen for soft, hydrated, three-dimensional conductive/ionic hydrogels, improving reproducibility and parameter comparability. Meanwhile, hydrogel iontronic devices may have electrochemical breakdown or leakage-channel amplification under low-frequency or large-signal situations, which must be detected and controlled using equivalent-circuit models (e.g., CPE plus leakage resistance) and frequency-dependent testing [92,124].

3.2.4. Ion-Gated Amplification and Programmable Transduction Pathways

EGTs are typical three-terminal ion-electron coupled devices (as illustrated in Figure 4c). EGTs use an ionically conductive but electrically insulating electrolyte, such as hydrogels, ionogels, or eutectogels, as the gate dielectric. Under low operating voltages, ion migration controls charge carriers in the semiconductor channel, allowing current amplification and programmable responses. The primary advantage is the creation of high-specific-capacitance EDL at the electrolyte/semiconductor interface. This allows the gadgets to consume less power, have greater mechanical flexibility, and be biocompatible at biological interfaces. As a result, EGTs are commonly used in neuromorphic synaptic devices and wearable or bioelectronic signal amplification [125–128]. This pathway is typically associated with hydrogel electrolytes or ionogels that can efficiently couple ionic transport in the soft phase with electronic modulation in an adjacent semiconductor channel.

Based on whether ions are allowed to enter the channel, the operating mechanisms can generally be simplified into two categories. (i) EDL-type (capacitive modulation): ions mostly collect at the interface to create an EDL,

resulting in surface buildup or depletion of charge carriers in the channel; this is essentially a nanoscale capacitive modulation with rapid response and low power consumption [125]. (ii) Electrochemical-type mechanisms, such as bulk doping/dedoping and OECTs, employ the injection of ions into the channel to alter its doping state and bulk conductivity, leading to stronger ion-electron coupling and higher transconductance. This makes it suitable as a front-end amplifier for biological signals or a synaptic plasticity emulation unit [129].

Hydrogel/polymer-electrolyte-gated neuromorphic transistors: PVA electrolyte-gated indium tin oxide (ITO) devices display synaptic-like plasticity behaviors such as paired-pulse facilitation and spike-timing-dependent features, exemplifying the canonical path of EDL gating to low-voltage plasticity [126].

Gel-electrolyte solid-state OECTs (shown in Figure 4d) arrays for flexible biointerfaces: photopatternable double-network gel electrolytes enable stretchable solid-state OECTs arrays that preserve electrical homogeneity during deformation and provide continuous ECG monitoring. This engineering process represents gel gating followed by solid-state integration and long-term conformal attachment [130].

System-level integration of gel-gated OECTs has reported flexible in-sensor computing circuits based on non-aqueous gel-gated OECTs, integrating ionic-gate amplification and signal processing within a single flexible platform and highlighting the trend toward device-circuit-application co-integration [131]. DES/eutectogel-gated OECTs for environmental stability: Eutectogels used as semi-solid electrolytes in OECTs improve operational stability and mechanical compliance without the need for encapsulation; comparative studies systematically have evaluated transient and steady-state performance against hydrogels and ionogels, demonstrating their promise for wearable applications [132].

In order to differentiate the signal transduction mechanisms of HBIS, this review offers a system for categorization. Key parameters, performance indicators, characterization techniques, and the response pathway are all included in the framework. Table 3 lists the four primary routes including electrical double-layer capacitance, OECTs, impedance response, and resistive response. This framework allows researchers to quickly determine the best response style for certain application needs. After that, they can do quantitative assessments using the proper semiconductor or electrochemical characterisation methods.

Table 3. Classification of Response Pathways and Characterization Methods for Hydrogel-Based Iontronic Sensors.

Path Type	Key Parameters	Impact Indicators	Testing Methods	Suitable Scenarios
Resistor response	σ, μ, c	Sensitivity, Linearity	IV curve, four-probe, CV	Static strain/pressure sensing, wearable motion monitoring, resistive sensors
Impedance Response	$Z_{j\omega}$, R_s, W	Lag, response time, Drift	EIS, Bode, Nyquist	Dynamic sensing, frequency-dependent analysis, drift-sensitive applications
EDL Capacitor	C_{dl}, τ = RC	Bandwidth, response rate	CV, Capacitive scanning, piezoelectric	High-sensitivity tactile/pressure sensors, iontronic skins, fast-response EDL devices
EGTs/OECTs	g_m, Doped conductivity	Gain, adjustability, hysteresis	IV, Pulse Scan, Capacitive Scan	Signal amplification, neuromorphic computing, bio-signal recording (ECG/EMG)

4. Stability and Biointerfacial Considerations

As hydrogel-based iontronic sensors move closer to real-world applications such as wearables, implantable devices, and environmental monitoring, environmental stability and interfacial compatibility are emerging as important barriers in engineering translation. Hydrogels have distinct advantages due to their high water content and soft-tissue-matched mechanics, but they are also more sensitive to humidity and temperature fluctuations, interfacial polarization, and complex in vivo chemical environments, resulting in signal drift, hysteresis, and noise [124]. This part examines the sources of stability and possible optimization strategies from three different perspectives: environmental adaptation, interfacial engineering, and multiphysics-coupled control.

4.1. Environmental Stability

4.1.1. Anti-Dehydration and Anti-Swelling Design

Hydrogels' high water content supports their ionic conductivity and mechanical compliance; however, in open environments, they are prone to dehydration and drying, which induce volumetric shrinkage, collapse of the porous network, and destabilization of ionic pathways, leading to rapid degradation of conductivity and sensitivity, whereas in high-humidity or immersed conditions, excessive swelling and interfacial hydrodynamic reorganization may occur, resulting in signal drift and reduced repeatability [124,133,134]. Therefore, improving environmental stability is not simply a matter of preventing water loss, but rather of balancing ionic transport, mechanical softness, and interfacial reliability under fluctuating humidity conditions.

To combat dehydration, low-volatility and wide-temperature-stable ionic-liquid-based ionogels are frequently used as alternatives or hybrid solutions, allowing for reasonably stable ionic conductivity and mechanical integrity under complex humidity conditions. For example, Shi et al. [32] reported a non-hygroscopic and humidity-insensitive ionogel (shown in Figure 5a) iontronic array that enabled intra-articular pressure monitoring, exemplifying a representative paradigm in which non-aqueous ionic conductors are used to improve long-term stability. However, although ionogels can effectively improve resistance to dehydration, replacing the aqueous phase may also influence the ionic conductivity and biointerfacial compatibility of the system. Therefore, the improved environmental stability of ionogels may be accompanied by some compromise in functional performance, depending on the application scenario.

In addition, DES/eutectogel systems, as well as nanocomposite reinforcement and encapsulation-based isolation techniques, have been used to prevent both dehydration and swelling. For example, Lu et al. [30] found that using a hydrophobic DES-based eutectogel (Figure 5d) increased long-term stability in high-humidity environments, demonstrating the relationship between solvent system selection to balance between water uptake and loss to signal stability. At the same time, strategies such as hydrophobic solvent design, nanocomposite reinforcement, or encapsulation may also introduce limitations, such as reduced interfacial compatibility, increased stiffness, or delayed response. Recent reviews have carefully reviewed the current design principles for anti-drying, anti-swelling, and anti-freezing conductive gels, which include solvent replacement, strong hydrogen bonding or ionic association, double-network designs, and encapsulation.

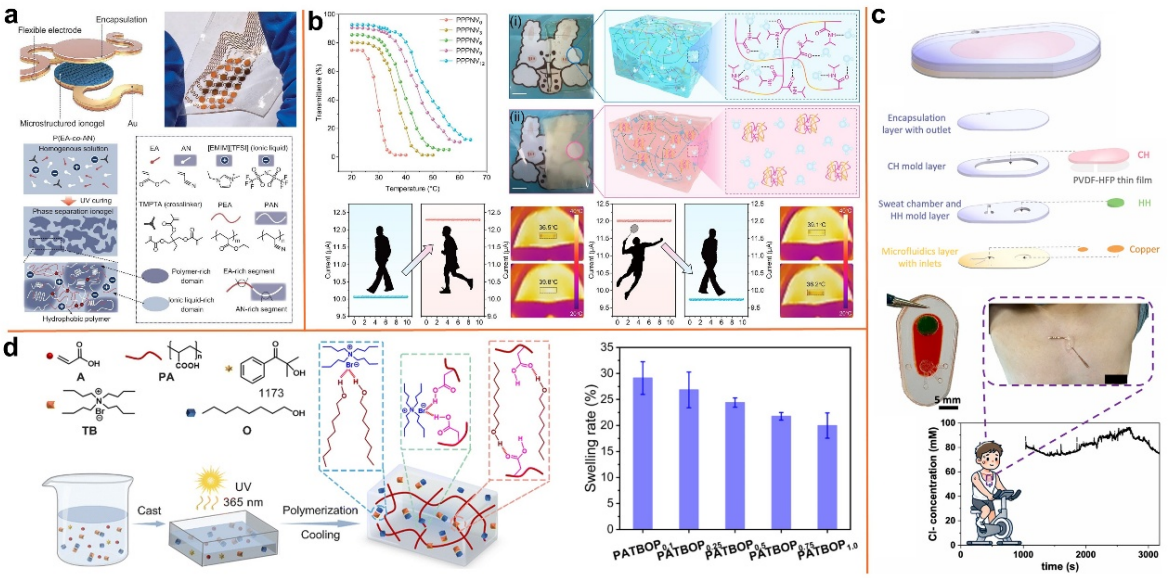

Figure 5. Construction of HBIS with Environmental Stability. Copyright 2022, Elsevier. (**a**) Network structure illustration of non-hygroscopic and humidity-insensitive ionogel [32]. Copyright 2024, Oxford University Press (OUP); (**b**) Illustration of network structure of PNIPAAm-based temperature responsive ionic conductive hydrogel [135]. Copyright 2025, Elsevier; (**c**) Schematic diagram of hydrogel-assisted interfaces in sweat-based systems for decrease lipid fouling and stabilize sensor outputs [102]. Copyright 2025, Elsevier; (**d**) Illustration of eutectogel with optimized multifunctionality and anti-swelling capabilities [30]. Copyright 2025, Royal Society of Chemistry (RSC).

4.1.2. Temperature Robustness and Drift Compensation

Temperature fluctuations affect both bulk ionic transport in hydrogels and the interfacial EDL structure. On the one hand, ionic mobility and the effective diffusion coefficient often grow with temperature and are frequently modeled by Arrhenius-type thermally activated behavior, resulting in systematic drift in conductivity and time-domain responses (rise and recovery durations). Temperature, on the other hand, affects solvent dielectric properties, solvation/desolvation equilibria, and interfacial adsorption, exacerbating the temperature dependence of EDL capacitance and polarization relaxation and increasing low-frequency hysteresis and noise [62,136–138].

The temperature dependence of ionic mobility/conductivity can often be approximated by an Arrhenius relationship. Temperature fluctuations may also cause changes in network microstructure in systems incorporating thermoresponsive polymers (lower critical solution temperature (LCST)/upper critical solution temperature (UCST)) or solvents with significant thermal expansion, resulting in nonlinear outputs and baseline drift.

Temperature-induced drift is typically caused by two mechanisms: (i) UCST/LCST phase transitions or segmental relaxation of polymer networks (e.g., nonlinear electrical responses induced by thermoresponsive backbones such as poly(N-isopropylacrylamide) (PNIPAAm)), and (ii) solvent thermal expansion and redistribution of water states that alter ionic-channel geometry and local viscosity (Figure 5b) [135]. To improve thermal robustness, the prevailing strategy is to transform the temperature-sensitive aqueous phase into a more stable ionic environment and implement compensation at both device and algorithmic levels: materials-wise, introducing organic solvents, ionic liquids, or deep eutectic solvents (forming organohydrogels, eutectogels, or ionogels), or incorporating nanofillers (e.g., MXene) can suppress freezing and thermally induced structural fluctuations, thereby maintaining stable coupling between conductivity and deformation at low temperatures; at the device level, temperature reference channels can be incorporated for calibration mapping; at the modeling level, temperature-dependent PNP/EDL models can be employed to predict drift trends and back-extract key parameters [42]. However, these strategies may also involve trade-offs, because improving thermal stability can sometimes increase material complexity or affect the original mechanical and electrical properties of the hydrogel system.

As representative examples, deep eutectic solvent systems such as ChCl:urea have been used to create eutectogel-based sensing materials that operate reliably at low temperatures. MXene-composited hydrogels are commonly used to improve low-temperature usability. For example, MXene-PAM/agar double-network strain sensors may operate at temperatures as low as −26 °C. Meanwhile, antifreezing ionic hydrogels based on glycerol/salt synergistic methods can maintain relatively strong ionic conductivity at even lower temperatures, establishing a material foundation for sustained signal readout over a wide temperature range [62].

4.1.3. Chemical Corrosion and Adaptability to Complex Media

In practical applications, hydrogel-based iontronic sensors are frequently exposed for extended periods of time to complex media such as perspiration, saliva, blood, or interstitial fluids, as well as external pollutants. Multicomponent ions, small organic molecules, proteins, and enzymes can interact with the hydrogel network or electrode interfaces via ion exchange, adsorption, and biochemical reactions, resulting in network degradation, aggravated interfacial polarization, and increased noise, ultimately reducing device lifetime [139,140]. In sweat or biofluid environments, common destabilization pathways include high-salinity-induced ion exchange and uncontrolled swelling, enzymatic or hydrolytic chain scission, protein adsorption-induced interfacial nonlinearity and enhanced electrode polarization, as well as contamination and performance drift caused by microbial adhesion [139,141].

Accordingly, improving chemical stability and tolerance to complex media should be understood as targeting three representative failure mechanisms: bulk network degradation, surface fouling, and biofouling-induced signal drift. Based on this framework, three complementary strategies are commonly employed. First, salt- and enzyme-resistant crosslinked or copolymerized networks are mainly intended to mitigate bulk degradation caused by ion exchange, hydrolysis, and enzymatic attack. Their working principle lies in increasing crosslinking stability and reducing the fraction of exchangeable or hydrolytically labile bonds, thereby preserving structural integrity and ionic transport pathways during prolonged exposure to harsh media. Their effectiveness is typically verified by accelerated aging tests in saline or enzyme-containing solutions, together with measurements of mechanical retention, swelling ratio, mass loss, and electrical stability. Second, antifouling interfacial layers, such as zwitterionic or strongly hydrated coatings, as well as filtration or barrier membranes, are primarily used to address surface fouling induced by proteins, lipids, and other contaminants. These interfaces usually function by forming highly hydrated and low-adhesion surface layers that suppress nonspecific adsorption and help maintain stable ion transport and interfacial impedance. Their performance is commonly validated by protein adsorption assays,

surface characterization methods such as contact-angle analysis or quartz crystal microbalance measurements, and long-term electrical stability tests in biofluid analogs. Third, antibacterial and regenerable interfaces, including silver nanoparticles, chitosan-based antimicrobial components, and self-healing coatings, are mainly introduced to suppress microbial colonization and biofilm formation, which otherwise lead to long-term drift and signal degradation. In addition to preventing bacterial growth, such interfaces may also facilitate functional recovery after contamination or mechanical damage. Their effectiveness is generally assessed through antibacterial assays, biofilm inhibition tests, and prolonged stability measurements in biologically active media [139,142].

Wearable sweat chloride-ion sensing: By including an ultrahydrophilic (poly(vinylidene fluoride-co-hexafluoropropylene) (PVDF-HFP)) membrane to limit ion exchange and hydrogel swelling, a more stable and reversible sensing response was obtained (as illustrated in Figure 5c) [102]. Nevertheless, these stabilization strategies may also affect ion transport or interfacial exchange to some extent, and therefore require a balance between chemical stability and sensing performance. Antifouling in sweat-based systems: To address signal degradation caused by lipid and organic interference in sweat, hydrogel-assisted interfaces have been used to decrease lipid fouling and stabilize sensor outputs, demonstrating an interfacial filtration/antifouling method [143]. Coatings with antibacterial and antifibrotic activities have been found to considerably reduce biofouling and immune-response-induced passivation of electrochemical performance in implantable and biofluid settings, paving the door for long-term in vivo monitoring [144]. These examples further illustrate that the choice of chemical-stabilization strategy should be guided by the dominant failure mechanism in the target medium, while its effectiveness should be evaluated through corresponding structural, interfacial, and electrical characterization methods.

4.2. Biointerface Engineering

4.2.1. Mechanical Coupling and Reversible Adhesive Interface Design

When using hydrogels for skin or tissue attachment, the main problem is to achieve modulus matching while also providing robust yet reversible interfacial adhesion, which reduces stress concentration, separation, and irritant responses. In general, adjusting the elastic modulus of hydrogels (Figure 6a) to be similar to that of soft tissues (usually in the tens of kilopascals, or 20–100 kPa) promotes conformal contact and extended use [145–149]. However, better modulus matching does not always guarantee the best overall performance, because excessively soft materials may sacrifice mechanical robustness during long-term use. The first method involves using biomimetic microstructures (such as octopus sucker arrays) to improve effective contact and shear resistance on rough or dynamic skin surfaces; for example, 3D-printed octopus-sucker-inspired hydrogels have been used in wearable sensing, demonstrating stable adhesion and sustained reliability in motion monitoring and ECG acquisition [150,151]. The second approach strengthens interfacial interactions via surface chemical adhesive groups, typically by introducing polydopamine (PDA) or polyamine/polylysine to provide reversible hydrogen bonding and coordination interactions, thereby maintaining low interfacial impedance and stable adhesion under dynamic conditions; for example, PDA-based tissue-adhesive layers have been integrated into functional hydrogel electronic skin patches for robust contact and extended operation on dynamic skin [152]. At the same time, stronger adhesion may also reduce reversibility or increase the risk of skin irritation during repeated attachment and detachment.

To reconcile strong adhesion on the skin-contacting side with anti-fouling/anti-unintended adhesion on the outer side, Janus (dual-faced asymmetric) interface designs have improved rapidly in recent years. Via integrated fabrication, one line of work creates single-sided sticky conductive hydrogels, providing interfacial mechanical stability during long-term dynamic monitoring. This idea has also been comprehensively characterized as a biointerface engineering framework with tissue-integration-promoting behavior on the substrate side and anti-adhesion/anti-wear properties on the top layer [153]. Although this type of design is advantageous for interfacial regulation, it may also increase structural and fabrication complexity.

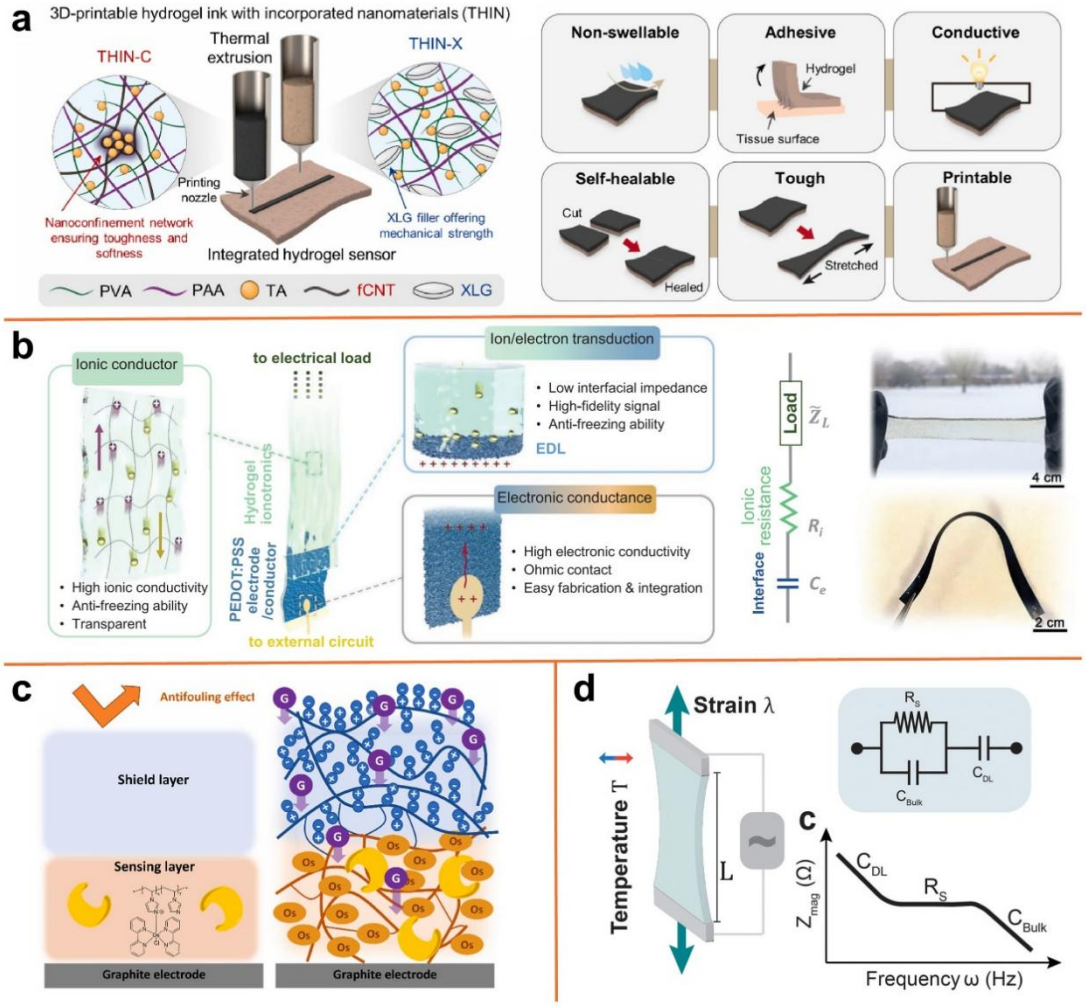

Figure 6. The HBIS with biointerface engineering design. (**a**) Network structure illustration of 3D-printable modulus-tunable hydrogel with multiple functionalities [145]. Copyright 2024, Elsevier; (**b**) Ionically-conductive hydrogel with a stable and low interfacial impedance and improved voltage tolerance [154]. Copyright 2022, Wiley-VCH ; (**c**) Schematic of a glucose biosensor enzyme gel electrode used for the evaluation of anti-fouling and sensing [155]. Copyright 2024, Elsevier; (**d**) Illustration of multiphysics coupling regulation for hydrogel [33]. Copyright 2023, RSC.

4.2.2. Polarization and Hysteresis at Electrochemical Interfaces

The hydrogel-electrode interface is the primary location for ion-electron coupling and signal transduction, but it is also the most susceptible to polarization, hysteresis, and low-frequency noise amplification. Common origins include electric field asymmetry caused by interfacial charge accumulation, mismatches between the formation/relaxation kinetics of the EDL and external stimuli, local depletion or enrichment arising from mismatches between fixed charge density and ionic distribution, as well as interfacial leakage and side reactions under long-term operation or large-signal excitation (Faradaic processes such as hydrogen or oxygen evolution may occur when the electrochemical window is exceeded), which ultimately manifest as baseline drift, nonlinearity, and non-overlapping response paths [124,156].

Interfacial charge co-design: by adjusting fixed charge density and ionic strength in hydrogels, the Debye length can be matched with electrode surface properties, eliminating hysteresis caused by concentration polarization and excessive electrostatic repulsion/adsorption [86]. Electrode material substitution and interfacial capacitance increase: Replacing traditional metals with high-capacitance, mechanically compliant conductive polymers or carbon-based electrodes (e.g., PEDOT:PSS, CNTs) can significantly lower interfacial impedance while improving signal quality and long-term stability (shown in Figure 6b) [154,157]. Suppression of side reactions via buffer/insulating layers: Introducing neutral buffer layers or confined electrolyte layers at the interface mitigates local pH shifts and Faradaic leakage; meanwhile, small-signal AC testing combined with equivalent circuit models (CPE plus leakage resistance) enables identification of low-frequency instability modes [124].

4.2.3. Biocompatibility and Immune Evasion Mechanisms

For implantable or long-term skin-adhered hydrogel iontronic devices, stable operation is frequently hampered by foreign body responses, in which nonspecific protein adsorption on material surfaces causes inflammatory cell adhesion and fibrotic encapsulation, resulting in impaired interfacial mass transport, signal attenuation, and drift [155]. As a result, the primary goal of biointerface engineering is to inhibit protein adsorption, limit cell adhesion and inflammatory cascades, and, where needed, establish long-term safety and maintainability via degradable or renewable outer layers [158].

Common immune-evasion techniques involve adding zwitterionic moieties at the interface to generate strongly hydrated layers, resulting in extremely low protein adsorption. Inert polymer shielding layers, such as poly(ethylene glycol) (PEG), are used to minimize cell adhesion and inflammation. To reduce the burden of foreign bodies over time, implantable devices incorporate degradable encapsulation or replaceable outer layers [158]. Biocompatibility assessment should adhere to the risk management framework, in which the most recent version, expressly incorporates biological evaluation into the risk management process [159].

Wareham-Mathiassen et al. [144] reported an implantable sensor coating with combined antibacterial and antifibrotic functions, which mitigates lifetime degradation caused by biofouling and fibrotic encapsulation, exemplifying an integrated strategy of anti-fouling plus immunomodulation. Another representative line of work involves tethering zwitterionic polymer coatings onto the surfaces of implantable electrochemical sensors, such as glucose sensors (Figure 6c), to reduce foreign body responses and protein fouling, demonstrating the direct benefits of zwitterionic strategies for long-term stability [155].

4.3. Multiphysics Coupling Regulation

Mechanical deformation, electric field driving, ionic diffusion/migration, and thermal fields (as well as porous fluid transport) frequently influence iontronic sensors in practice. Hysteresis, drift, and frequency dependence are often caused by the coupled feedback between these processes, which cannot be adequately described by a single-physics model. As a result, developing systematic multiphysics coupling models is an important tool for understanding mechanisms and designing predictive devices [160].

4.3.1. Integrated Modeling Framework

In practical applications, iontronic sensors are frequently subjected to a combination of mechanical loads, electric fields, diffusion, and thermal fields, which makes it challenging for a single-physics model to adequately describe their behavior. As a result, creating systematic multiphysics coupling models has become an indispensable tool for mechanistic research and predictive device design.

4.3.2. Multiphysics Coupling Models

Previous research has combined the PNP framework with chemical processes (ionic activity and osmotic pressure), mechanical responses (swelling and large deformation), and thermal fields (temperature-dependent mobility and diffusion) to jointly predict ion distributions, electric potential evolution, and volumetric or deformation changes in hydrogels, thereby more comprehensively explaining sensor outputs and drift origins under pressure and temperature perturbations [33,161]. Typical examples are Stewart et al. [160] reported electro-chemical-mechanical finite-deformation theory, which provides a unified modeling framework for capacitive strain sensing and large-strain actuation in ionic hydrogels.

For example, Balakrishnan et al. [33] used PNP to generate simulated impedance spectra under strain and temperature variations (Figure 6d), revealing quantitative relationships between frequency, sensitivity, and structural length scales and demonstrating a modeling pathway from fundamental mechanisms to device-level readouts. Recent multiphysics numerical methods have moved beyond traditional mesh-based finite element approaches to mesh-independent or remeshing-free frameworks in order to accommodate huge deformations and significant geometric nonlinearities. For instance, meshless multiphysics systems based on maximum-entropy interpolation may manage massive deformations and instabilities without requiring frequent remeshing, increasing simulation robustness under complex operating conditions [161]. Meanwhile, an increasing number of studies combine swelling with external flow or permeation into a coherent mechanical framework, resulting in a more consistent representation of the interconnected problems of deformation, convection, and ionic redistribution [162].

Meanwhile, data-driven techniques are emerging as a complement to electrochemical modeling. By combining multifrequency EIS data with physically interpretable representations such as the DRT, and subsequently applying recurrent neural networks for time-series prediction, multiscale hysteresis and drift

behaviors can be characterized and compensated, thereby improving the efficiency of long-term stability assessment [163]. Standardized DRT analytic methodologies and open-source tools have also been improved in recent years, resulting in a more reusable implementation foundation for closed-loop processes that include testing, modeling, and algorithmic compensation [164].

This part examines the stability constraints of hydrogel-based iontronic sensors in complex environments and biointerfaces, summarizing the primary failure paths and engineering options. On the environmental side, the focus is on resistance to dehydration and excessive swelling, response consistency under temperature changes, and suppression of chemical corrosion and contamination in complicated media. On the interfacial side, the emphasis is on tissue modulus matching and reversible adhesion, as well as the regulation of polarization and hysteresis at electrode-hydrogel interfaces. Methodologically, electro-chemo-thermo-mechanical multiphysics coupling models and data-driven analyses are used to understand drift and hysteresis and to promote predictive design. Collectively, these approaches work together to achieve a single goal: to integrate material formulation, interface engineering, and model calibration into a closed-loop framework that allows for the development of long-term stable, reliable, and quantifiable iontronic sensors, as well as their translation from the laboratory to clinical and industrial applications [124,160,165].

5. Applications and Devices

HBIS has evolved from fundamental studies of material systems and ion transport into a rapidly expanding application-oriented field. Benefiting from their softness, stretchability, processability, and compatibility with wet biological interfaces, hydrogel-based iontronic systems offer clear advantages over conventional rigid electronics in conformal biointegration, interfacial electrochemical coupling, and multiphysical signal acquisition. In parallel, ionogels and eutectogels have emerged as important complementary platforms for long-term operation and harsh or complex environments because of their low volatility, high ionic conductivity, and broad environmental tolerance [56]. From an application perspective, the performance of HBIS is governed by the coupling among material system, dominant ion transport mechanism, and signal transduction pathway. Wearable and implantable bioelectronics mainly rely on diffusion- and electromigration-dominated transport together with low-impedance interfacial modulation; soft robotics and human-machine interfaces more strongly involve deformation-induced ion redistribution and EDL regulation; environmental and food monitoring often depends on analyte-, humidity-, or temperature-induced perturbations in ionic distribution and interfacial polarization; and self-powered devices exploit directed ion migration and interfacial charge modulation under external gradients. Accordingly, the following sections discuss representative applications not simply as device examples, but as manifestations of mechanism-guided optimization of hydrogel composition, microstructure, interface, and architecture.

5.1. Wearable Physiological Monitoring

Wearable health monitoring is one of the most advanced applications of hydrogel-based iontronic sensing, allowing for continuous and non-invasive gathering of bioelectrical and mechanical information. Hydrogel electrolytes and ionic conductors can generate low-interfacial-impedance, mechanically conformal soft electrode-skin interfaces on the skin surface, boosting signal quality and comfort. Meanwhile, conductive polymer hydrogels are widely used for electrochemical detection and continuous monitoring of epidermal chemical information, such as sweat electrolytes and pH levels [166,167]. Choline-based solutions, for example, have gained popularity due to their low toxicity and environmental stability. Early research by the Mecerreyes group [168] identified cholinium-based ionogels as solid-state skin-electrode electrolyte interfaces, allowing for stable ECG recording for up to 72 h while lowering skin impedance to levels equivalent to commercial Ag/AgCl electrodes. In wearable physiological monitoring, the dominant mechanisms are usually diffusion and electromigration of mobile ions within hydrated conductive networks, together with impedance reduction and EDL modulation at the soft skin–electrode interface. Accordingly, material design in this class of devices is mainly optimized toward high ionic conductivity, low interfacial impedance, wet adhesion, and resistance to dehydration or interfacial drift. Therefore, ion-conductive hydrogels, eutectogels, and ionogels are particularly suitable because they can maintain stable ion transport while preserving conformal contact with dynamic skin surfaces.

More recent research has extended long-term stability to more demanding use situations. For example, a cholinium-based eutectogel electrode described in De la et al. [169] provided high-quality continuous electroencephalography (EEG)/ECG recording under dynamic conditions (with demonstrations lasting more than 48 h), demonstrating the interfacial durability of gel electrodes during motion. Li et al. [170] fabricated an ion-conducting, sweat-resistant bioelectronic skin sensor (SRBSS) with strong wet adhesion (Figure 7a). MXene nanosheets enhanced the sensing response and reduced the interfacial impedance at physiologically relevant

electrical frequencies. The high conductivity of the SRBSS mainly relies on mobile ions (Li+ and Cl−), enabling reliable electrical signal readout. Here, the incorporation of MXene mainly serves to reduce interfacial impedance and improve signal fidelity, illustrating how nanocomposite design can be used to optimize the same transport and transduction processes for wearable recording. On the other hand, to address interfacial drift and dehydration caused by sweat and humid conditions, Liu et al. [171] proposed sweat-activated conductive hydrogel nanomesh electrodes (as displayed in Figure 8a**)** that enabled ultralong-term epidermal bioelectrical recording (with demonstrations approaching ~100 days). This example highlights that, beyond intrinsic conductivity, long-term wearable performance also depends on structural and interfacial engineering that stabilizes ionic transport under realistic conditions. It should be noted that the key bottlenecks of wearable systems remain water loss, interfacial polarization or drift, and packaging durability; thus, synergistic optimization of material formulations (water retention/anti-swelling), interfacial structures (low-impedance soft electrodes), and encapsulation strategies is critical to the viability of long-term monitoring [172].

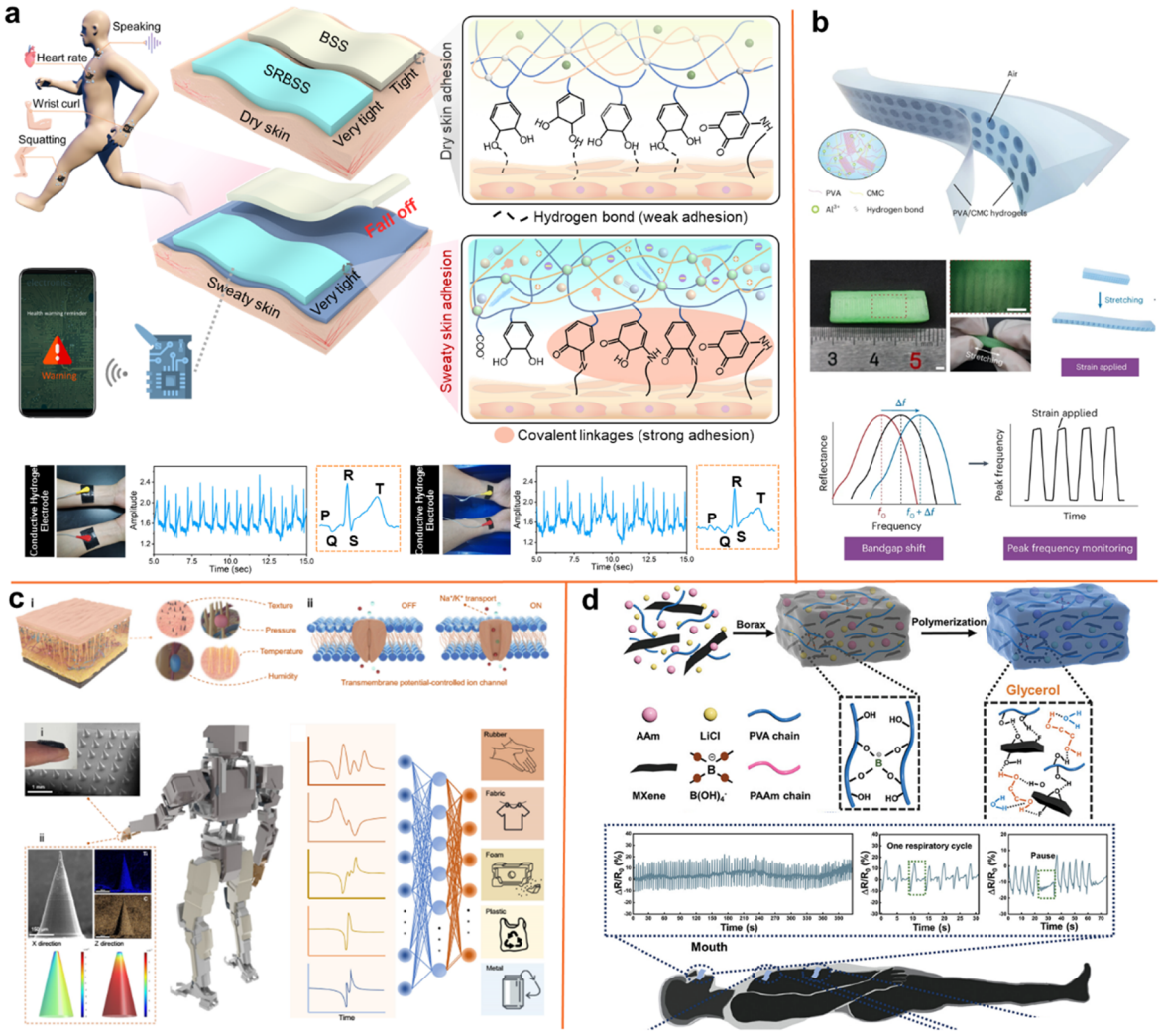

Figure 7. HBIS applications that span monitoring human motions, implantable biosensing, human-machine interaction, robotic electronic skin, and physiological signals. (**a**) Schematic illustration showing wearable physiological monitoring with hydrogel device [170]. Copyright 2022, Cell Press; (**b**) Schematic diagram of the injectable or absorbable hydrogel-acoustic device [173]. Copyright 2025, Springer Nature; (**c**) Schematic illustration depicting soft robotics and human-machine interfaces with microstructured hydrogel [174]. Copyright 2025, Springer Nature; (**d**) Schematic diagram of flexible sensor to monitor breathing state [175]. Copyright 2024, Wiley-VCH.

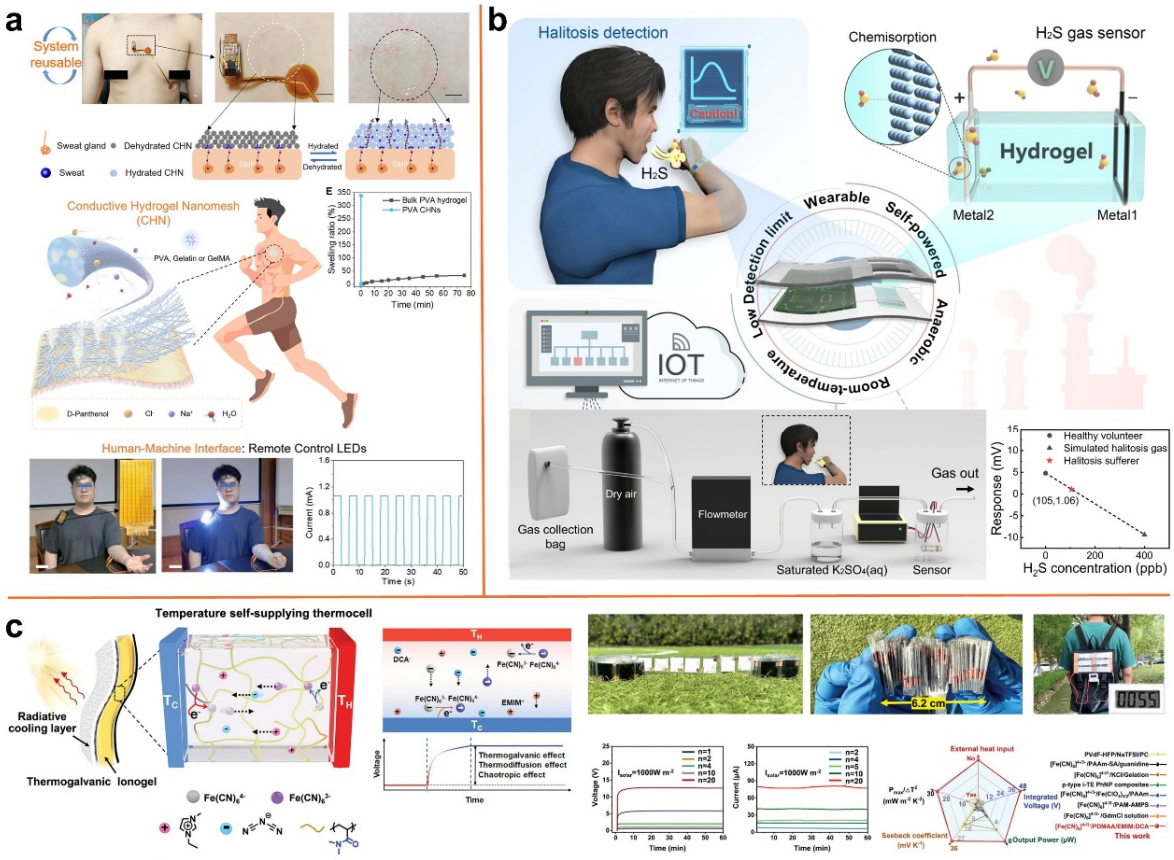

Figure 8. HBIS applications that span human-machine interaction, environment monitoring and energy conversion. (**a**) Schematic illustration showing the nanomesh-reinforced hydrogel electrodes for electrophysiological monitoring and human-centric interactions [171]. Copyright 2026, Cell Press; (**b**) Schematic diagram of the flexible sensing device and its application in H_2S leakage alarm [176]. Copyright 2023, Springer Nature; (**c**) Schematic depicting the hydrogel electrodes for harvest energy [177]. Copyright 2024, Wiley-VCH.

5.2. Implantable and In Vivo Biosensing

In contrast to epidermal devices, implantable hydrogel ion-electron sensors must maintain long-term stable performance in complicated in vivo conditions, putting greater emphasis on mechanical compatibility, biocompatibility, signal robustness, and long-term safety. Because of their high water content and tissue-like elastic moduli, hydrogels reduce inflammation caused by mechanical mismatch, making them promising candidates for long-term in vivo sensing applications. Recent research has revealed highly compliant, attachable, or biodegradable hydrogel-based devices capable of continuously monitoring in vivo signals such as tissue strain, cavity pressure or flow, and bioelectrical activity. For implantable and in vivo biosensing, diffusion and electromigration remain the fundamental ion-transport processes, but the dominant design challenge shifts from short-term signal generation to long-term transport stability, interfacial robustness, and suppression of biological drift. In this context, the relevant signal transduction pathways are often impedance-based, electrochemical, or wireless readout modes that are strongly influenced by tissue–device coupling, interfacial polarization, and biofouling. As a result, material and structural optimization in implantable systems places greater emphasis on ultrasoft mechanics, tissue adhesion, biocompatibility, encapsulation, and stable signal transmission under complex in vivo conditions.

Tian et al. [173] reported an all-hydrogel phononic crystal implanted strain sensor (as displayed in Figure 7b). By modulating ultrasonic reflection bandgaps via periodic cavity/air-column architectures, the device enables continuous and wireless monitoring of internal tissue strain, with validation demonstrated in large animals (pigs), highlighting an alternative strategy that replaces traditional rigid electronics with a soft-structure acoustic readout. Another representative direction is in vivo multimodal monitoring using ultrasoft plus tissue-adhesive structures. Oh et al. [178] reported an ultrasoft, tissue-adhesive hydrogel-based implantable device that concurrently captures bladder deformation and electromyographic signals, proving in vivo practicality in anesthetized pig models. Furthermore, research on injectable or absorbable hydrogel-acoustic devices is growing, resulting in structural paradigms and material design references for minimally invasive implantation and wireless readout [179]. Despite

these advances, implantable applications are still limited by long-term stability, immune responses or fibrotic encapsulation, packaging, and in vivo calibration, emphasizing the need for coordinated optimization of materials, interfaces, and readout systems, as well as more extensive preclinical testing [180,181].

5.3. Soft Robotics and Human-Machine Interfaces

Soft robotics and human-machine interfaces (HMIs) place strict requirements on sensing layers, such as high compliance, multidimensional deformation readability, and high cyclic stability, in order to produce high-fidelity signals under dynamic conditions such as grasping, bending, shear, and rapid contact. Hydrogel- or ionogel-based iontronic sensors rely on ion migration and EDL modulation to provide low-modulus conformability, stretchability, and processability, allowing for continuous tactile-deformation feedback on soft actuator surfaces. Multimodal decoupling of pressure and strain signals, as well as array-based readout, can be achieved by designing ionic transport channels and interfacial microstructures inside the gel, enabling HMI systems such as glove-type inputs, soft robotic skins, and wearable control interfaces (as presented in Figure 7c) [174]. Representative examples include the biomimetic ion-mechanoreceptive skin reported by Amoli et al. [182], which integrate iontronic skin arrays with flexible circuitry to achieve real-time control of drone flight direction and speed, demonstrating the system-level viability of ionic skins for soft interactive control. Another common line of work uses transparent and self-healing ionogel strain arrays to detect small deformations such as eye movements, which are then applied to human-machine control of unmanned systems. In soft robotics and human-machine interfaces, the core functional requirement is to convert dynamic mechanical deformation into readable electrical signals with high fidelity. Therefore, these applications are mainly governed by deformation-induced ionic redistribution, diffusion/electromigration-coupled impedance variation, and interfacial EDL modulation; under rapid loading or microstructured confinement, convective contributions may also become important. Correspondingly, microstructured surfaces, engineered ionic channels, array architectures, and self-healing or highly stretchable gel systems are commonly adopted to enhance sensitivity, decouple multiple mechanical inputs, and maintain stable cyclic performance.

Recent ionogel reviews have highlighted corresponding device paradigms and essential material combinations, such as silica scaffolds synergistically coupled with ionic liquids to form conductive and elastic frameworks, as examples of HMI methods [56]. Meanwhile, emerging biomimetic microstructured piezoionic strategies are advancing artificial tactile units with higher recognition accuracy; for example, Ding et al. [174] used skin-inspired structural enhancement to improve the trade-off between sensitivity and stability in ionically conductive hydrogel tactile units, resulting in transferable structural templates for soft robotic skins and high-precision inputs.

5.4. Environmental and Food Quality Monitoring

The advantages of hydrogel- and ionogel-based iontronic devices lie in environmental and food quality monitoring, including deployable soft interfaces, high ionic coupling sensitivity, and ease of integration with wireless or distributed systems. By incorporating molecular recognition elements into the gel network, such as specific coordination or reactive sites, molecular imprinting motifs, photoelectroactive probes, or fluorescent/colorimetric groups, target-induced changes in ionic distribution and interfacial EDL states can be converted into electrical signals (e.g., resistance, impedance, or capacitance) or optical readouts, allowing for rapid in situ detection in complex environments. Environmental and food quality monitoring applications are more strongly associated with analyte-induced perturbation of ionic distribution, adsorption/interfacial polarization, and humidity- or temperature-dependent ionic transport. Accordingly, their dominant signal transduction pathways are usually resistive, impedance, capacitive, electrochemical, or, in some cases, self-powered outputs. To optimize these mechanisms, material design often incorporates selective recognition motifs, adsorption-active interfaces, porous encapsulation, or environmentally stable ionogels/organohydrogels, so that changes in gas composition, humidity, dissolved species, or temperature can be efficiently converted into measurable electrical signals.

In gas and volatile biomarker monitoring, ionogels or water-rich ionic conductors can convert ion-channel disturbances caused by trace gases into readable signals. For example, Ni et al. [175] reported a stretchable self-powered H_2S sensor (as presented in Figure 7d) employed a water-rich ionically conductive hydrogel system, demonstrating feasibility for non-invasive diagnosis of oral malodor (associated with bacterial-metabolism-derived H_2S) and early detection of meat spoilage, thereby illustrating a direct mapping between environmental or food gas biomarkers, ionic flux, and device output. Similarly, for environmental parameters such as oxygen or dissolved oxygen, researchers have developed hydrogel-based oxygen sensors encapsulated in porous elastomers,

allowing for stable operation across a wide range of environments and integration with wireless modules for real-time monitoring of respiration-related and ambient oxygen levels.

For humidity, respiration, or storage-transport microenvironment monitoring, hydrogels have high sensitivity to water activity, making them ideal for developing sensing pathways based on humidity-ionic conductivity/interfacial polarization-impedance response. Ni et al. [175] reported an environmentally robust organic hydrogel humidity sensor leveraging a double-network design and the synergistic combination of LiCl and MXene exhibited high sensitivity and rapid response across respiration-relevant humidity levels, highlighting its promise for wearable devices and food storage or logistics monitoring.

In temperature and extreme-condition monitoring, ionogels are commonly used for thermal and multiparameter sensing in firegrounds, high-temperature settings, and other severe conditions due to their low volatility and large operational range. In recent years, ionogel temperature sensors and systems built for harsh circumstances have been reported, with a focus on gel-ionic liquid or gel-salt coupling as a pathway to stable and linearly calibrable thermal responses [183]. Furthermore, ionogel microneedle arrays have been designed for wearable mechano-thermal multimodal sensing, resulting in a structured-channel and ion-modulation device framework ideal for fire, deep-sea, and aerospace applications [184].

5.5. Energy Conversion and Self-Powered Devices

Recent efforts to reduce reliance on external power and improve sustained operation in wearable and remote sensing applications have emphasized the monolithic integration of energy conversion modules with hydrogel or ionogel sensing layers, allowing devices to function in a closed-loop manner across energy harvesting, power delivery, and signal readout. The embeddable conversion mechanisms primarily include triboelectric nanogenerator (TENG)-driven contact-separation energy harvesting, ion thermoelectric or thermogalvanic outputs driven by thermal gradients, and hydrovoltaic or moist-electric power generation caused by water gradients, humidity adsorption, and interfacial charge modulation. Fundamentally, these processes rely on ion movement and redistribution within gel networks and interfacial electric double layers, which directly transfer mechanical, thermal, or chemical potential differences into detectable electrical signals and allow for self-powered, self-driven sensing [185]. Huang et al. [176] reported self-powered H_2S biomarker sensors (as presented in Figure 8b) based on a battery-like architecture that leverages intrinsically stretchy (organic) hydrogel electrolytes to ensure long-term stable operation. Applications include detecting oral malodor and meat rotting. In energy conversion and self-powered devices, the core mechanism is the directional migration and redistribution of ions under external gradients, such as mechanical contact-separation, thermal gradients, or moisture gradients. In this case, the transduction process extends beyond passive sensing and directly converts ion transport and interfacial charge modulation into voltage or current output through triboelectric, thermogalvanic, hydrovoltaic, or moist-electric pathways. Therefore, material and structural design is typically optimized through redox-active ionogels, double-network hydrogel electrodes, interfacial charge-regulation strategies, and gradient-engineered architectures, which together enhance energy-conversion efficiency while preserving flexibility and sensing functionality.

Ou et al. [186] used double-network hydrogel electrodes to create triboelectric nanogenerators that can harvest energy while also sensing strain or pressure. In terms of thermal energy usage, thermoelectrochemical hydrogel fiber devices combine thermogalvanic effects with piezoresistive responses, employing the output current to achieve self-powered pressure sensing and demonstrating a thermo-electro-mechanical multiphysics device route [187,188]. At the level of ambient energy harvesting, studies and reviews on moist-electric or hydrovoltaic generation show that directional ion migration caused by surface charges and moisture gradients can produce long-term electrical output, providing new power supply options for low-power sensing nodes [185,189]. Yan et al. [177] (Figure 8c) discussed device architecture as well as ionogel electrolyte design. A redox-type ionogel with an exceptionally high thermal voltage of 32.4 mV/K was found. Under natural circumstances, the thermoelectric cell can create an internal temperature gradient by incorporating radiative cooling technology. Solar energy is selectively shielded or absorbed to create this gradient. Consequently, the apparatus provides consistent power output in a variety of environmental circumstances.

In conclusion, hydrogel-based iontronic sensors have demonstrated clear functional differences across a variety of application domains. Wearable applications promote non-invasive operation, continuous signal capture, and low interfacial impedance [190]. Implantable in vivo monitoring focuses on mechanical compatibility with soft tissues, long-term biocompatibility, and wireless readout. Soft robotics and human-machine interfaces use high compliance, multimodal coupling, and cyclic stability to provide skin-like tactile and deformation input. Environmental and food monitoring prioritizes selectivity and prompt on-site reaction. Energy conversion and self-powered techniques seek to integrate ionic transport and energy harvesting into a single device architecture,

minimizing reliance on external power sources and increasing system autonomy. Examples include human-machine interfaces that use iontronic skin arrays to achieve gesture- and pressure-based control of drones via ion-pair pumping and EDL transduction [182]. An all-hydrogel ultrasonic metagel implantable strain sensor allows for continuous wireless monitoring of interior tissue strain via phononic crystal bandgap alterations [173]. Self-powered H_2S sensors using stretchable solid electrolytes have been created for non-invasive halitosis diagnosis and early detection of meat deterioration [176]. Furthermore, thorough evaluations and viewpoints on self-powered processes and device techniques help establish a structured framework for sensor-energy integration [185]. Future research priorities are expected to shift from incremental material performance enhancement to interpretable multiphysics coupling mechanisms, integrated and manufacturable device and packaging designs, standardized, comparable evaluation, and real-world validation to support clinical and industrial deployment [29].

6. Conclusions and Outlook

This review summarizes recent advances in the material systems, ion transport mechanisms, signal transduction pathways, and representative applications of HBIS (Figure 9). At the materials level, polyelectrolyte hydrogels, ionic liquids, ionogels/eutectogels, and nanocomposite hydrogels provide complementary advantages in fixed-charge regulation, environmental stability, and coupled mechanical-electrical enhancement, collectively driving the field beyond single-parameter optimization toward integrated materials design that balances conductivity, mechanical robustness, stability, bandwidth, and interfacial adaptability [12].

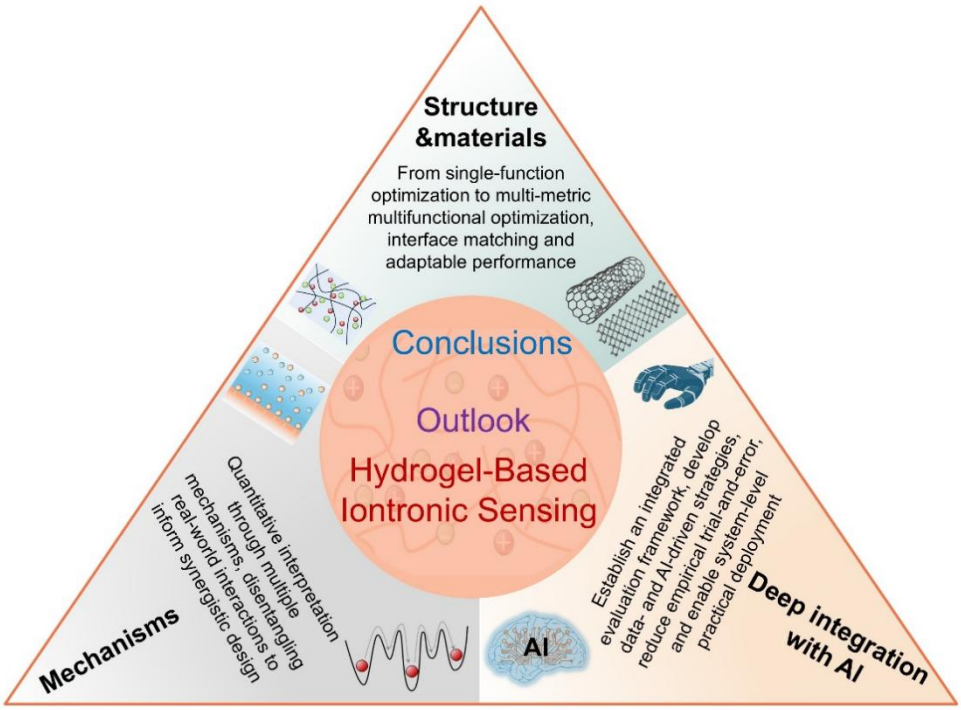

Figure 9. Conclusion and Perspective of HBIS.

At the mechanistic level, the macroscopic response of HBIS is governed not by an isolated process, but by the coupled interplay of diffusion, electromigration, electro-osmotic flow/convection, electric-double-layer reorganization, and adsorption/desorption processes across both bulk and interface. Incorporation of these processes into PNP-based analysis and EIS-supported quantitative frameworks provides a mechanistic basis for linking structure, transport, and function, and thus offers practical design handles for tuning sensitivity, response speed, operational bandwidth, hysteresis, and long-term drift [12].

Furthermore, two significant obstacles to long-term use are stability and biointerface behavior. Thermal drift, swelling, and environmental drying all happen at the same time. They alter the hydrogel's ion mobility and interfacial polarization. Thus, low-frequency noise rises. In the meantime, biointerface problems directly affect the safety and dependability of devices. The contact may be harmed by a biomechanical mismatch. To guarantee long-term stability, these components (including moisture-barrier encapsulation, ionic liquid or organic solvent substitution, interfacial buffer layers, and electrode material optimization) must be co-designed. The readout strategy must be supported by these material selections. Signal-to-noise ratio can be enhanced by lock-in detection.

When combined, they aid in maintaining signal constancy in complicated media and under long-term cyclic loading [12].

Intelligent HBIS devices have gained prominence due to the quick development of artificial intelligence (AI) technologies. As research advances, HBIS has progressed past a phase focused on structural improvement and performance tweaking. Its potential for next-generation wearable technology is further enhanced by the fact that it is about to enter an era of integration and intelligence. Simultaneously, raw electrical outputs can be converted into useful information using AI-driven techniques. They allow for the delicate decoding of minute variations in the resistive, capacitive, or triboelectric signals that hydrogels produce. In systems connected with mechanical metamaterials that incorporate programmed deformation modes, for example, this advantage is maintained even in situations when the mechanical response is extremely complicated.

Beyond these challenge-driven directions, hybrid modeling and AI-assisted design are expected to further accelerate the field. Multiphysics models that integrate deformation, electric field, diffusion, thermal, and fluidic effects can improve predictive capability and reduce reliance on empirical trial-and-error optimization. In parallel, data-driven analysis and generative design may enable more efficient optimization of polymer composition, crosslinking architecture, and device geometry. However, the value of these approaches lies not merely in computational sophistication, but in their ability to improve interpretability, standardization, long-term reliability, and translational practicality.

Overall, the next stage of HBIS development will likely be defined by the convergence of mechanism-guided material design, standardized evaluation, and manufacturable system integration. With continued advances along these directions, HBIS is expected to evolve from laboratory-scale demonstrations into robust, intelligent, and application-ready iontronic platforms for biomedical monitoring, environmental sensing, and human-machine interfacing.

Author Contributions

W.L.: writing—original draft preparation, data curation, visualization; S.W.: data curation, writing—reviewing and editing; Y.S.: conceptualization, supervision, writing—reviewing and editing; J.L.: conceptualization, supervision, writing-reviewing and editing; J.Z.: conceptualization, supervision, writing—reviewing and editing. All authors have read and agreed to the published version of the manuscript.

Funding

This work was supported by the Natural Science Foundation of Xiamen (3502Z202571063), the Natural Science Foundation of Fujian Province (2025J08130), the Talents Introduction Program of Xiamen University of Technology (YKJ24043R), the Natural Science Foundation of Jiangsu Province (BK20250495), the Jiangsu Funding Program for Excellent Postdoctoral Talent (2025ZB354), and the China Postdoctoral Science Foundation (2024M763174).

Institutional Review Board Statement

Not applicable.

Informed Consent Statement

Not applicable.

Data Availability Statement

Data will be made available on request.

Conflicts of Interest

The authors declare no conflict of interest.

Use of AI and AI-Assisted Technologies

No AI tools were utilized for this paper.

References

1. Zhang, J.; Wang, M. Alternative Micro/Nanofabrication Approaches for Wearable Electronics. *Chem. Rev.* **2026**, *126*, 1686–1762. https://doi.org/10.1021/acs.chemrev.5c00801.

2. Luo, Y.; Abidian, M.R.; Ahn, J.-H.; et al. Technology roadmap for flexible sensors. *ACS Nano* **2023**, *17*, 5211–5295. https://doi.org/10.1021/acsnano.2c12606.
3. Tang, W.; Sun, Q.; Wang, Z.L. Self-powered sensing in wearable electronics—A paradigm shift technology. *Chem. Rev.* **2023**, *123*, 12105–12134. https://doi.org/10.1021/acs.chemrev.3c00305.
4. Niu, Y.; Liu, H.; He, R.; et al. The new generation of soft and wearable electronics for health monitoring in varying environment: From normal to extreme conditions. *Mater. Today* **2020**, *41*, 219–242. https://doi.org/10.1016/j.mattod.2020.10.004.
5. Zhao, C.; Park, J.; Root, S.E.; et al. Skin-inspired soft bioelectronic materials, devices and systems. *Nat. Rev. Bioeng.* **2024**, *2*, 671–690. https://doi.org/10.1038/s44222-024-00194-1.
6. Wang, Y.; Haick, H.; Guo, S.; et al. Skin bioelectronics towards long-term, continuous health monitoring. *Chem. Soc. Rev.* **2022**, *51*, 3759–3793. https://doi.org/10.1039/d2cs00207h.
7. Park, J.; Lee, Y.; Cho, S.; et al. Soft sensors and actuators for wearable human–machine interfaces. *Chem. Rev.* **2024**, *124*, 1464–1534. https://doi.org/10.1021/acs.chemrev.3c00356.
8. Hou, Y.; Hou, X. Bioinspired nanofluidic iontronics. *Science* **2021**, *373*, 628–629. https://doi.org/10.1126/science.abj0437.
9. Ro, Y.G.; Na, S.; Kim, J.; et al. Iontronics: Neuromorphic Sensing and Energy Harvesting. *ACS Nano* **2025**, *19*, 24425–24507. https://doi.org/10.1021/acsnano.5c04885.
10. Yoo, H.; Lee, Y.H.; Lee, M.-G.; et al. Gel-Based Ionic Circuits. *Chem. Rev.* **2025**, *125*, 8956–9011. https://doi.org/10.1021/acs.chemrev.5c00245.
11. Yuan, H.; Zhang, Q.; Cheng, Y.; et al. Double-sided microstructured flexible iontronic pressure sensor with wide linear sensing range. *J. Colloid Interface Sci.* **2024**, *670*, 41–49. https://doi.org/10.1016/j.jcis.2024.05.054.
12. Zhu, J.; Tao, J.; Yan, W.; et al. Pathways toward wearable and high-performance sensors based on hydrogels: Toughening networks and conductive networks. *Natl. Sci. Rev.* **2023**, *10*, nwad180. https://doi.org/10.1093/nsr/nwad180.
13. Roy, A.; Afshari, R.; Jain, S.; et al. Advances in conducting nanocomposite hydrogels for wearable biomonitoring. *Chem. Soc. Rev.* **2025**, *54*, 2595–2652. https://doi.org/10.1039/d4cs00220b.
14. Li, W.; Zhou, R.; Ouyang, Y.; et al. Harnessing biomimicry for controlled adhesion on material surfaces. *Small* **2024**, *20*, 2401859. https://doi.org/10.1002/smll.202401859.
15. Li, Y.; Bai, N.; Chang, Y.; et al. Flexible iontronic sensing. *Chem. Soc. Rev.* **2025**, *54*, 4651–4700. https://doi.org/10.1039/d4cs00870g.
16. Wang, Z.; Wei, H.; Huang, Y.; et al. Naturally sourced hydrogels: Emerging fundamental materials for next-generation healthcare sensing. *Chem. Soc. Rev.* **2023**, *52*, 2992–3034. https://doi.org/10.1039/d2cs00813k.
17. Li, W.; Guan, Q.; Li, M.; et al. Nature-inspired strategies for the synthesis of hydrogel actuators and their applications. *Prog. Polym. Sci.* **2023**, *140*, 101665. https://doi.org/10.1016/j.progpolymsci.2023.101665.
18. Choi, S.-G.; Kang, S.-H.; Lee, J.-Y.; et al. Recent advances in wearable iontronic sensors for healthcare applications. *Front. Bioeng. Biotechnol.* **2023**, *11*, 1335188. https://doi.org/10.3389/fbioe.2023.1335188.
19. Mo, F.; Lin, Y.; Liu, Y.; et al. Advances in ionic conductive hydrogels for skin sensor applications. *Mater. Sci. Eng. R Rep.* **2025**, *165*, 100989. https://doi.org/10.1016/j.mser.2025.100989.
20. Chen, W.; Zhai, L.; Zhang, S.; et al. Cascade-heterogated biphasic gel iontronics for electronic-to-multi-ionic signal transmission. *Science* **2023**, *382*, 559–565. https://doi.org/10.1126/science.adg0059.
21. Gao, N.; Pan, C. Intelligent ion gels: Design, performance, and applications. *SmartMat* **2024**, *5*, e1215. https://doi.org/10.1002/smm2.1215.
22. Chen, X.; Xia, X.; Guo, C.F. Flexible iontronic sensing: Ionic materials, electrodes, and encapsulation. *Adv. Funct. Mater.* **2025**, *36*, e12920. https://doi.org/10.1002/adfm.202512920.
23. Liu, Q.; Liu, Z.; Li, C.; et al. Highly transparent and flexible iontronic pressure sensors based on an opaque to transparent transition. *Adv. Sci.* **2020**, *7*, 2000348. https://doi.org/10.1002/advs.202000348.
24. Boateng, D.; Li, X.; Zhu, Y.; et al. Recent advances in flexible hydrogel sensors: Enhancing data processing and machine learning for intelligent perception. *Biosens. Bioelectron.* **2024**, *261*, 116499. https://doi.org/10.1016/j.bios.2024.116499.
25. Lee, J.; Ihle, S.J.; Pellegrino, G.S.; et al. Stretchable and suturable fibre sensors for wireless monitoring of connective tissue strain. *Nat. Electron.* **2021**, *4*, 291–301. https://doi.org/10.1038/s41928-021-00557-1.
26. Zhao, C.; Wang, Y.; Tang, G.; et al. Ionic flexible sensors: Mechanisms, materials, structures, and applications. *Adv. Funct. Mater.* **2022**, *32*, 2110417. https://doi.org/10.1002/adfm.202110417.
27. Chen, J.; Zhu, Y.; Chang, X.; et al. Recent progress in essential functions of soft electronic skin. *Adv. Funct. Mater.* **2021**, *31*, 2104686. https://doi.org/10.1002/adfm.202104686.
28. Schroeder, T.B.; Guha, A.; Lamoureux, A.; et al. An electric-eel-inspired soft power source from stacked hydrogels. *Nature* **2017**, *552*, 214–218. https://doi.org/10.1038/nature24670.
29. Choi, K.; Lee, G.; Lee, M.-G.; et al. Bio-Inspired Ionic Sensors: Transforming Natural Mechanisms into Sensory Technologies. *Nano-Micro Lett.* **2025**, *17*, 180. https://doi.org/10.1007/s40820-025-01692-6.

30. Lu, Q.; Li, H.; Cai, C.; et al. Hydrophobic deep eutectic solvent-based eutectogels for long-term humidity resistance and multifunctional sensing. *Mater. Horiz.* **2025**, *12*, 9801–9807. https://doi.org/10.1039/d5mh01293g.
31. Cui, X.; Xi, Y.; Tu, S.; et al. An overview of flexible sensors from ionic liquid-based gels. *TrAC Trends Anal. Chem.* **2024**, *174*, 117662. https://doi.org/10.1016/j.trac.2024.117662.
32. Shi, J.; Xie, S.; Liu, Z.; et al. Non-hygroscopic ionogel-based humidity-insensitive iontronic sensor arrays for intra-articular pressure sensing. *Natl. Sci. Rev.* **2024**, *11*, nwae351. https://doi.org/10.1093/nsr/nwae351.
33. Balakrishnan, G.; Song, J.; Khair, A.S.; et al. Poisson–Nernst–Planck framework for modelling ionic strain and temperature sensors. *J. Mater. Chem. B* **2023**, *11*, 5544–5551. https://doi.org/10.1039/d2tb02819k.
34. Lu, D.; Chen, H. Solid-state organic electrochemical transistors (OECTs) based on gel electrolytes for biosensors and bioelectronics. *J. Mater. Chem. A* **2025**, *13*, 136–157. https://doi.org/10.1039/d4ta05288a.
35. Yang, C.; Suo, Z. Hydrogel ionotronics. *Nat. Rev. Mater.* **2018**, *3*, 125–142. https://doi.org/10.1038/s41578-018-0018-7.
36. Yiming, B.; Guo, X.; Ali, N.; et al. Ambiently and mechanically stable ionogels for soft ionotronics. *Adv. Funct. Mater.* **2021**, *31*, 2102773. https://doi.org/10.1002/adfm.202102773.
37. Yuk, H.; Lu, B.; Zhao, X. Hydrogel bioelectronics. *Chem. Soc. Rev.* **2019**, *48*, 1642–1667. https://doi.org/10.1039/c8cs00595h.
38. Liu, X.; Liu, J.; Lin, S.; et al. Hydrogel machines. *Mater. Today* **2020**, *36*, 102–124. https://doi.org/10.1016/j.mattod.2019.12.026.
39. Li, G.; Li, C.; Li, G.; et al. Development of conductive hydrogels for fabricating flexible strain sensors. *Small* **2022**, *18*, 2101518. https://doi.org/10.1002/smll.202101518.
40. Zhou, C.; Wu, T.; Xie, X.; et al. Advances and challenges in conductive hydrogels: From properties to applications. *Eur. Polym. J.* **2022**, *177*, 111454. https://doi.org/10.1016/j.eurpolymj.2022.111454.
41. Hou, W.; Sheng, N.; Zhang, X.; et al. Design of injectable agar/NaCl/polyacrylamide ionic hydrogels for high performance strain sensors. *Carbohydr. Polym.* **2019**, *211*, 322–328. https://doi.org/10.1016/j.carbpol.2019.01.094.
42. Zhang, D.; Chen, H.; Zhang, Y.; et al. Antifreezing hydrogels: From mechanisms and strategies to applications. *Chem. Soc. Rev.* **2025**, *54*, 5292–5341. https://doi.org/10.1039/d4cs00718b.
43. Liza, L.; Kabir, M.H.; Kabir, M.; et al. Flexible fabric-integrated PAAm–LiCl hydrogel pressure sensor for wearable and soft robotics applications. *Mater. Adv.* **2025**, *6*, 9590–9601. https://doi.org/10.1039/d5ma00942a.
44. Zheng, B.; Zhou, H.; Zhao, G.; et al. Bioinspired electrically conductive hydrogels: Rational engineering for next-generation flexible mechanosensors. *Mater. Sci. Eng. R Rep.* **2025**, *166*, 101080. https://doi.org/10.1016/j.mser.2025.101080.
45. Hu, L.; Chee, P.L.; Sugiarto, S.; et al. Hydrogel-based flexible electronics. *Adv. Mater.* **2023**, *35*, 2205326. https://doi.org/10.1002/adma.202205326.
46. Wang, J.; Chen, Y.; Tu, S.; et al. Recent advances in flexible iontronic pressure sensors: Materials, microstructure designs, applications, and opportunities. *J. Mater. Chem. C* **2024**, *12*, 14202–14221. https://doi.org/10.1039/d4tc03226h.
47. He, Y.; Cheng, Y.; Yang, C.; et al. Creep-free polyelectrolyte elastomer for drift-free iontronic sensing. *Nat. Mater.* **2024**, *23*, 1107–1114. https://doi.org/10.1038/s41563-024-01848-6.
48. Song, J.; Yang, R.; Shi, J.; et al. Polyelectrolyte-based wireless and drift-free iontronic sensors for orthodontic sensing. *Sci. Adv.* **2025**, *11*, eadu6086. https://doi.org/10.1126/sciadv.adu6086.
49. Fan, X.; Chen, Z.; Sun, H.; et al. Polyelectrolyte-based conductive hydrogels: From theory to applications. *Soft Sci.* **2022**, *2*, 10. https://doi.org/10.20517/ss.2022.09.
50. Pan, X.; Wang, Q.; Benetti, D.; et al. Polyelectrolyte hydrogel: A versatile platform for mechanical-electric conversion and self-powered sensing. *Nano Energy* **2022**, *103*, 107718. https://doi.org/10.1016/j.nanoen.2022.107718.
51. Wang, Z.; Si, Y.; Zhao, C.; et al. Flexible and washable poly (ionic liquid) nanofibrous membrane with moisture proof pressure sensing for real-life wearable electronics. *ACS Appl. Mater. Interfaces* **2019**, *11*, 27200–27209. https://doi.org/10.1021/acsami.9b07786.
52. Chen, S.; Zhang, M.; Zou, P.; et al. Historical development and novel concepts on electrolytes for aqueous rechargeable batteries. *Energy Environ. Sci.* **2022**, *15*, 1805–1839. https://doi.org/10.1039/d2ee00004k.
53. Liu, J.; Liu, X.; Chen, J.; et al. Drying-enhanced polyvinyl alcohol-polyacrylic acid double-network hydrogel and its application in flexible strain sensors. *Chem. Eng. Sci.* **2022**, *264*, 118120. https://doi.org/10.1016/j.ces.2022.118120.
54. Liu, Z.; Wang, Y.; Ren, Y.; et al. Poly (ionic liquid) hydrogel-based anti-freezing ionic skin for a soft robotic gripper. *Mater. Horiz.* **2020**, *7*, 919–927. https://doi.org/10.1039/c9mh01688k.
55. Ji, R.; Yan, S.; Zhu, Z.; et al. Ureido-Ionic Liquid Mediated Conductive Hydrogel: Superior Integrated Properties for Advanced Biosensing Applications. *Adv. Sci.* **2024**, *11*, 2401869. https://doi.org/10.1002/advs.202401869.
56. Fan, X.; Liu, S.; Jia, Z.; et al. Ionogels: Recent advances in design, material properties and emerging biomedical applications. *Chem. Soc. Rev.* **2023**, *52*, 2497–2527. https://doi.org/10.1039/d2cs00652a.
57. Nie, B.; Li, R.; Cao, J.; et al. Flexible transparent iontronic film for interfacial capacitive pressure sensing. *Adv. Mater.* **2015**, *27*, 6055–6062. https://doi.org/10.1002/adma.201502556.
58. Wang, X.; Guo, C.; Su, Z.; et al. Flexible iontronic pressure sensing technology: Advanced structural ionic layer. *Iontronics* **2026**, *2*, 1. https://dx.doi.org/10.20517/iontronics.2026.01.

59. Zhang, Y.-A.; Ma, K.; Chen, K.-Z.; et al. Flexible wearable ionogels: Classification, fabrication, properties and applications. *Sens. Actuators A Phys.* **2024**, *372*, 115325. https://doi.org/10.1016/j.sna.2024.115325.
60. Wen, J.; Zhou, L.; Ye, T. Polymer ionogels and their application in flexible ionic devices. *SmartMat* **2024**, *5*, e1253. https://doi.org/10.1002/smm2.1253.
61. Xiong, Y.; Han, J.; Wang, Y.; et al. Emerging iontronic sensing: Materials, mechanisms, and applications. *Research* **2022**, *2022*, 9867378. https://doi.org/10.34133/2022/9867378.
62. Hu, X.; Zhao, Y.; Pu, L.; et al. Stretchable anti-freeze deep eutectic solvent (DES) gels for low-temperature wearable soft sensors. *New J. Chem.* **2024**, *48*, 11003–11013. https://doi.org/10.1039/d4nj00452c.
63. Htwe, Y.Z.N.; Pawłowska, S.; Jaafar, M. Emerging Strategies for the Fabrication of Conductive Hydrogels from Conductive Polymers and Their Composites for Wearable Sensors, Energy Storage, and Biosensor Applications: Methods, Mechanisms, and Future Perspectives. *Adv. Mater. Technol.* **2025**, *11*, e01845. https://doi.org/10.1002/admt.202501845.
64. Zhu, T.; Ni, Y.; Biesold, G.M.; et al. Recent advances in conductive hydrogels: Classifications, properties, and applications. *Chem. Soc. Rev.* **2023**, *52*, 473–509. https://doi.org/10.1039/d2cs00173j.
65. Ren, J.; Wang, Y.; Liu, Z.; et al. Balancing stretchability and conductivity: Carbon nanotube layer-enhanced non-ionic conductive hydrogels with a sandwich structure. *Chem. Eng. J.* **2024**, *500*, 156641. https://doi.org/10.1016/j.cej.2024.156641.
66. Hauck, M.; Saure, L.M.; Zeller-Plumhoff, B.; et al. Overcoming water diffusion limitations in hydrogels via microtubular graphene networks for soft actuators. *Adv. Mater.* **2023**, *35*, 2302816. https://doi.org/10.1002/adma.202370292.
67. Lin, Y.; Wu, A.; Zhang, Y.; et al. Recent progress of nanomaterials-based composite hydrogel sensors for human–machine interactions. *Discov. Nano* **2025**, *20*, 1–30. https://doi.org/10.1186/s11671-025-04240-8.
68. Li, W.; Liu, J.; Wei, J.; et al. Recent progress of conductive hydrogel fibers for flexible electronics: Fabrications, applications, and perspectives. *Adv. Funct. Mater.* **2023**, *33*, 2213485. https://doi.org/10.1002/adfm.202213485.
69. Peng, Q.; Chen, J.; Wang, T.; et al. Recent advances in designing conductive hydrogels for flexible electronics. *InfoMat* **2020**, *2*, 843–865. https://doi.org/10.1002/inf2.12113.
70. Guan, Z.; Jiang, Y.; Zhou, Y.; et al. Liquid metal-based electrodes for flexible electronics: Z. Guan et al. *Rare Met.* **2025**, *44*, 6897–6923. https://doi.org/10.1007/s12598-025-03466-w.
71. Li, Y.; Zhao, Y.; Yang, R.; et al. Flexible electrodes with enhancement of electronic-ionic conductivity for electrophysiological signal monitoring. *Wearable Electron.* **2024**, *1*, 228–235. https://doi.org/10.1016/j.wees.2024.09.005.
72. Liu, K.; Duan, T.; Zhang, F.; et al. Flexible electrode materials for emerging electronics: Materials, fabrication and applications. *J. Mater. Chem. A* **2024**, *12*, 20606–20637. https://doi.org/10.1039/d4ta01960a.
73. Yan, N.; Sujanani, R.; Kamcev, J.; et al. Salt and ion transport in a series of crosslinked AMPS/PEGDA hydrogel membranes. *J. Membr. Sci.* **2022**, *653*, 120549. https://doi.org/10.1016/j.memsci.2022.120549.
74. Dai, Q.; Liao, W.; Liu, J.; et al. Microfluidic bubble-templating 3D printing of ordered macroporous hydrogels. *Compos. Part B Eng.* **2024**, *284*, 111725. https://doi.org/10.1016/j.compositesb.2024.111725.
75. Yang, Z.; Wang, J.; Wan, X.; et al. Microbubble-based fabrication of resilient porous ionogels for high-sensitivity pressure sensors. *Microsyst. Nanoeng.* **2024**, *10*, 177. https://doi.org/10.1038/s41378-024-00780-8.
76. Adelnia, H.; Ensandoost, R.; Moonshi, S.S.; et al. Freeze/thawed polyvinyl alcohol hydrogels: Present, past and future. *Eur. Polym. J.* **2022**, *164*, 110974. https://doi.org/10.1016/j.eurpolymj.2021.110974.
77. Nordness, O.; Moon, J.D.; Marioni, N.; et al. Probing water and ion diffusion in functional hydrogel membranes by PFG-NMR. *Macromolecules* **2023**, *56*, 4669–4680. https://doi.org/10.1021/acs.macromol.3c00306.
78. Yu, Y.Y.; Xiang, H.P.; Fan, L.F.; et al. Shape Memory Elastomers: A Review of Molecular Structures, Stimulus Mechanisms, and Emerging Applications. *Polym. Sci. Technol.* **2025**, *1*, 271–298. https://doi.org/10.1021/polymscitech.4c00035.
79. Fong, K.D.; Self, J.; McCloskey, B.D.; et al. Ion correlations and their impact on transport in polymer-based electrolytes. *Macromolecules* **2021**, *54*, 2575–2591. https://doi.org/10.1021/acs.macromol.0c02545.
80. Shao, Y.; Gudla, H.; Mindemark, J.; et al. Ion transport in polymer electrolytes: Building new bridges between experiment and molecular simulation. *Acc. Chem. Res.* **2024**, *57*, 1123–1134. https://doi.org/10.1021/acs.accounts.3c00791.
81. Kiyohara, K.; Tamura, M. Transport coefficients of gel electrolytes: A molecular dynamics simulation study. *J. Chem. Phys.* **2022**, *156*, 084905. https://doi.org/10.1063/5.0081118.
82. Lu, M.; Lian, W.Z.; Xiao, Z.; et al. Interplay of chain dynamics and ion transport on mechanical behavior and conductivity in ionogels. *Soft Matter* **2025**, *21*, 435–447. https://doi.org/10.1039/d4sm01251h.
83. Klika, V.; Gaffney, E.A. Upscaling the Poisson–Nernst–Planck equations for ion transport in weakly heterogeneous charged porous media. *Appl. Math. Lett.* **2023**, *137*, 108482. https://doi.org/10.1016/j.aml.2022.108482.
84. Appel, E.A.; Tibbitt, M.W.; Greer, J.M.; et al. Exploiting electrostatic interactions in polymer–nanoparticle hydrogels. *ACS Macro Lett.* **2015**, *4*, 848–852. https://doi.org/10.1021/acsmacrolett.5b00416.
85. Appel, E.A.; Tibbitt, M.W.; Webber, M.J.; et al. Self-assembled hydrogels utilizing polymer–nanoparticle interactions. *Nat. Commun.* **2015**, *6*, 6295. https://doi.org/10.1038/ncomms7295.

86. Ouyang, Y.; Wang, Z.L.; Wei, D. Ionic rectification via electrical double layer modulation at hydrogel interfaces. *RSC Appl. Interfaces* **2025**, *2*, 873–896. https://doi.org/10.1039/d5lf00098j.
87. Liu, Z.; Zheng, S.; Li, Z.; et al. Multiscale modeling of hydrogels. In *The Mechanics of Hydrogels*, Elsevier: Amsterdam, The Netherlands, 2022; pp. 187–222. http://dx.doi.org/10.1016/b978-0-08-102862-9.00012-9.
88. Shen, K.-H.; Fan, M.; Hall, L.M. Molecular dynamics simulations of ion-containing polymers using generic coarse-grained models. *Macromolecules* **2021**, *54*, 2031–2052. https://doi.org/10.1021/acs.macromol.0c02557.
89. Singhal, A.; Schneible, J.D.; Lilova, R.L.; et al. A multiscale coarse-grained model to predict the molecular architecture and drug transport properties of modified chitosan hydrogels. *Soft Matter* **2020**, *16*, 10591–10610. https://doi.org/10.1039/d0sm01243b.
90. Wang, M. Ionogels: From Properties and Synthesis to Toughening, Patterning, and Applications. *Chem. Rev.* **2025**, *125*, 11815–11839. https://doi.org/10.1021/acs.chemrev.5c00370.
91. Ouyang, Y.; Li, X.; Du, Y.; et al. Mechano-Driven Neuromimetic Logic Gates Established by Geometrically Asymmetric Hydrogel Iontronics. *Small* **2025**, *21*, 2409998. https://doi.org/10.1002/smll.202409998.
92. Daso, R.E.; Posey, R.; Garza, H.; et al. Standardized Electrochemical Characterization of Conductive Hydrogels. *Adv. Funct. Mater.* **2025**, *35*, e08859. https://doi.org/10.1002/adfm.71976.
93. Sun, W.; Xu, Z.; Qiao, C.; et al. Antifreezing proton zwitterionic hydrogel electrolyte via ionic hopping and grotthuss transport mechanism toward solid supercapacitor working at −50° C. *Adv. Sci.* **2022**, *9*, 2201679. https://doi.org/10.1002/advs.202201679.
94. Guo, Y.; Bae, J.; Fang, Z.; et al. Hydrogels and hydrogel-derived materials for energy and water sustainability. *Chem. Rev.* **2020**, *120*, 7642–7707. https://doi.org/10.1021/acs.chemrev.0c00345.
95. Zhang, S.; Song, C.; Ji, Z.; et al. Synergistic vehicular-grotthuss conduction in double-network hydrogel electrolytes for zinc dendrite suppression in zinc-air batteries. *J. Colloid Interface Sci.* **2026**, *703*, 139064. https://doi.org/10.1016/j.jcis.2025.139064.
96. Colla, T.; Telles, I.M.; Arfan, M.; et al. Spiers Memorial Lecture: Towards understanding of iontronic systems: Electroosmotic flow of monovalent and divalent electrolyte through charged cylindrical nanopores. *Faraday Discuss.* **2023**, *246*, 11–46. https://doi.org/10.1039/d3fd00062a.
97. Schuszter, G.; Gehér-Herczegh, T.; Szűcs, Á.; et al. Determination of the diffusion coefficient of hydrogen ion in hydrogels. *Phys. Chem. Chem. Phys.* **2017**, *19*, 12136–12143. https://doi.org/10.1039/c7cp00986k.
98. Barbero, G.; Lelidis, I. Analysis of Warburg's impedance and its equivalent electric circuits. *Phys. Chem. Chem. Phys.* **2017**, *19*, 24934–24944. https://doi.org/10.1039/c7cp04032f.
99. Henrique, F.; Gupta, A. Parallel Warburg Elements Describe Ionic Transport in Nanopores. *PRX Energy* **2025**, *4*, 023009. https://doi.org/10.1103/prxenergy.4.023009.
100. Xu, Z.; Yue, P.; Feng, J.J. Hystereses in flow-induced compression of a poroelastic hydrogel. *Soft Matter* **2024**, *20*, 6940–6951. https://doi.org/10.1039/d4sm00678j.
101. Biutty, M.N.; Kim, H.; Handayani, P.L.; et al. Self-powered smart pressure sensors by stimuli-responsive ion transport within layered hydrogels. *Chem. Eng. J.* **2024**, *495*, 153565. https://doi.org/10.1016/j.cej.2024.153565.
102. Zhang, W.; Zhang, X.; Dutta, A.; et al. Hydrogel-based sweat chloride sensor with high sensitivity and low hysteresis. *Biosens. Bioelectron.* **2025**, *288*, 117805. https://doi.org/10.1016/j.bios.2025.117805.
103. Liu, C.; Liu, Z. Micro-Gas Flow Sensor Utilizing Surface Network Density Regulation for Humidity-Modulated Ion Transport. *Gels* **2025**, *11*, 570. https://doi.org/10.3390/gels11080570.
104. Wu, M.; Liu, Z.; Gao, Y. Design and Fabrication of Microelectrodes for Dielectrophoresis and Electroosmosis in Microsystems for Bio-Applications. *Micromachines* **2025**, *16*, 190. https://doi.org/10.3390/mi16020190.
105. Wang, G.; Kato, K.; Aoki, I.; et al. Transdermal drug delivery using a porous microneedle device driven by a hydrogel electroosmotic pump. *J. Mater. Chem. B* **2024**, *12*, 1490–1494. https://doi.org/10.1039/d3tb02208k.
106. Kusama, S.; Sato, K.; Matsui, Y.; et al. Transdermal electroosmotic flow generated by a porous microneedle array patch. *Nat. Commun.* **2021**, *12*, 658. https://doi.org/10.1038/s41467-021-20948-4.
107. Zhu, K.; Luo, J.; Zhang, D.; et al. Molecular engineering enables hydrogel electrolyte with ionic hopping migration and self-healability toward dendrite-free zinc-metal anodes. *Adv. Mater.* **2024**, *36*, 2311082. https://doi.org/10.1002/adma.202311082.
108. Popov, I.; Zhu, Z.; Singh, H.; et al. Mechanisms of proton transport in aqueous acid solutions. *Cell Rep. Phys. Sci.* **2024**, *5*, 102294. https://doi.org/10.1016/j.xcrp.2024.102294.
109. Li, Z.; Yun, H.; Yan, Y.; et al. Boosting Electronic Charge Transport in Conductive Hydrogels via Rapid Ion-Electron Transduction. *Angew. Chem. Int. Ed.* **2025**, *64*, e202506560. https://doi.org/10.1002/ange.202506560.
110. Popov, I.; Zhu, Z.; Young-Gonzales, A.R.; et al. Search for a Grotthuss mechanism through the observation of proton transfer. *Commun. Chem.* **2023**, *6*, 77. https://doi.org/10.1038/s42004-023-00878-6.
111. Ichikawa, T.; Yamada, T.; Aoki, N.; et al. Surface proton hopping conduction mechanism dominant polymer electrolytes created by self-assembly of bicontinuous cubic liquid crystals. *Chem. Sci.* **2024**, *15*, 7034–7040. https://doi.org/10.1039/d4sc01211a.

112. Wang, Z.D.; Yang, Y.Q.; Chen, J.H.; et al. Proton Superhighways Enabled by Hofmeister-Electrostatic Synergy in All-Inorganic Polyoxometalate Hydrogels for Electronics. *Adv. Mater.* **2025**, *38*, e15892. https://doi.org/10.1002/adma.202515892.
113. Yang, H.; Sun, X.; Li, X.; et al. Janus Grotthuss-Vehicle Mechanism Enhances Fast OH− Transport for Ultralong Lifetime Flexible Zinc–Air Battery. *Adv. Funct. Mater.* **2024**, *34*, 2409695. https://doi.org/10.1002/adfm.202409695.
114. Chen, K.; Hu, H.; Song, I.; et al. Organic optoelectronic synapse based on photon-modulated electrochemical doping. *Nat. Photonics* **2023**, *17*, 629–637. https://doi.org/10.1038/s41566-023-01232-x.
115. Lazanas, A.; Simón, B.P. A guide to recognizing your electrochemical impedance spectra: Revisions of the randles circuit in (bio) sensing. *Sensors* **2025**, *25*, 6260. https://doi.org/10.3390/s25196260.
116. Plank, C.; Rüther, T.; Jahn, L.; et al. A review on the distribution of relaxation times analysis: A powerful tool for process identification of electrochemical systems. *J. Power Sources* **2024**, *594*, 233845. https://doi.org/10.1016/j.jpowsour.2023.233845.
117. Huang, Y.; Hu, S.; Li, Y.; et al. Programmable high-sensitivity iontronic pressure sensors support broad human-interactive perception and identification. *npj Flex. Electron.* **2025**, *9*, 41. https://doi.org/10.1038/s41528-025-00420-9.
118. Greco, A.; Imoto, S.; Backus, E.H.; et al. Ultrafast aqueous electric double layer dynamics. *Science* **2025**, *388*, 405–410. https://doi.org/10.1126/science.adu5781.
119. Yan, H.; Qi, R.; Liu, Z.; et al. Unlocking the potential of hydrogel-electrode electrical double layer for high-performance moisture-enabled electric generators. *Device* **2025**, *3*, 100568. https://doi.org/10.1016/j.device.2024.100568.
120. Gateman, S.M.; Gharbi, O.; De Melo, H.G.; et al. On the use of a constant phase element (CPE) in electrochemistry. *Curr. Opin. Electrochem.* **2022**, *36*, 101133. https://doi.org/10.1016/j.coelec.2022.101133.
121. Gamry Instruments. *Two-, Three-, and Four-Electrode Experiments*; Gamry Instruments: Warminster, PA, USA, 2021.
122. Jjagwe, J.; Olupot, P.W.; Kulabako, R.; et al. Electrochemical sensors modified with iron oxide nanoparticles/nanocomposites for voltammetric detection of Pb (II) in water: A review. *Heliyon* **2024**, *10*, e29743. https://doi.org/10.1016/j.heliyon.2024.e29743.
123. Lazanas, A.C.; Prodromidis, M.I. Electrochemical impedance spectroscopy—A tutorial. *ACS Meas. Sci. Au* **2023**, *3*, 162–193. https://doi.org/10.1021/acsmeasuresciau.2c00070.
124. Jiang, Y.; Han, Y.; Gao, Z.; et al. Frequency-dependent electrochemical breakdown of hydrogel ionotronics. *Extrem. Mech. Lett.* **2024**, *71*, 102210. https://doi.org/10.1016/j.eml.2024.102210.
125. Li, S.; Gao, L.; Liu, C.; et al. Biomimetic Neuromorphic Sensory System via Electrolyte Gated Transistors. *Sensors* **2024**, *24*, 4915. https://doi.org/10.3390/s24154915.
126. Huang, Y.J.; Di, J.K.; Li, Y.; et al. Polyvinyl alcohol electrolyte-gated oxide transistors with tetanization activities for neuromorphic computing. *J. Mater. Chem. C* **2024**, *12*, 5166–5174. https://doi.org/10.1039/d4tc00526k.
127. Owyeung, R.E.; Zeng, W.; Panzer, M.J.; et al. Free form three dimensional integrated circuits and wearables on a thread using organic eutectogel gated electrochemical transistors. *arXiv* **2023**, arXiv:2303.02447.
128. Wu, B.; Peng, Y.; Gao, L.; et al. Eutectogel-gated ultra-flexible organic electrochemical transistors for humidity sensing and neuromorphic computing. *Sens. Actuators B Chem.* **2025**, *450*, 139268. https://doi.org/10.1016/j.snb.2025.139268.
129. Tian, Z.; Zhao, Z.; Yan, F. Organic electrochemical transistor in wearable bioelectronics: Profiles, applications, and integration. *Wearable Electron.* **2024**, *1*, 1–25. https://doi.org/10.1016/j.wees.2024.03.002.
130. Tang, L.; Zheng, X.; Sun, M.; et al. Photopatternable gel electrolytes for stretchable solid-state organic electrochemical transistors. *Sci. China Mater.* **2025**, *68*, 3212–3218. https://doi.org/10.1007/s40843-025-3429-x.
131. Tian, X.; Bai, J.; Liu, D.; et al. A fully-integrated flexible in-sensor computing circuit based on gel-gated organic electrochemical transistors. *npj Flex. Electron.* **2025**, *9*, 90. https://doi.org/10.1038/s41528-025-00472-x.
132. Zhong, Y.; Lopez-Larrea, N.; Alvarez-Tirado, M.; et al. Eutectogels as a semisolid electrolyte for organic electrochemical transistors. *Chem. Mater.* **2024**, *36*, 1841–1854. https://doi.org/10.1021/acs.chemmater.3c02385.
133. Li, Y.; Cheng, Q.; Deng, Z.; et al. Recent progress of anti-freezing, anti-drying, and anti-swelling conductive hydrogels and their applications. *Polymers* **2024**, *16*, 971. https://doi.org/10.3390/polym16070971.
134. Fan, Z.; Ji, D.; Kim, J. Congelation-and dehydration-tolerant, mechanically robust hydrogel electrolyte for durable iontronic sensors operating in open air and freezing temperatures over wide strain and pressure ranges. *Chem. Eng. J.* **2024**, *499*, 156677. https://doi.org/10.1016/j.cej.2024.156677.
135. Lei, T.; Wang, Y.; Feng, Y.; et al. PNIPAAm-based temperature responsive ionic conductive hydrogels for flexible strain and temperature sensing. *J. Colloid Interface Sci.* **2025**, *678*, 726–741. https://doi.org/10.1016/j.jcis.2024.09.131.
136. Zhen, E.; Chen, Y.; Huang, J. Double-layer capacitance peaks: Origins, ion dependence, and temperature effects. *J. Chem. Phys.* **2025**, *162*, 144702. https://doi.org/10.1063/5.0251548.
137. De Bortoli, A.; Negro, E.; Di Noto, V. Generalized modified Poisson–Nernst–Planck model for electrical double layer with steric, correlation and thermal effects applied to fuel cells. *Electrochim. Acta* **2025**, *525*, 146070. https://doi.org/10.1016/j.electacta.2025.146070.
138. Chen, K.; Lai, W.; Xiao, W.; et al. Low-temperature adaptive dual-network mxene nanocomposite hydrogel as flexible wearable strain sensors. *Micromachines* **2023**, *14*, 1563. https://doi.org/10.3390/mi14081563.

139. Song, Z.; Han, R.; Yu, K.; et al. Antifouling strategies for electrochemical sensing in complex biological media. *Microchim. Acta* **2024**, *191*, 138. https://doi.org/10.1007/s00604-024-06218-2.
140. Wang, Z.; Liu, X.; Zhu, M.; et al. Recent advances in zwitterionic hydrogels: Structure, applications and challenges. *J. Mater. Chem. A* **2025**, *13*, 13693–13705. https://doi.org/10.1039/d5ta01111f.
141. Han, X.; Su, J.; Li, J.; et al. Bio-Inspired and Protein-Based Elastomeric Materials. *Polym. Sci. Technol.* **2025**, *2*, 6–21. https://doi.org/10.1021/polymscitech.5c00054.
142. Zhang, T.; Liang, X.; Wang, L.; et al. An ionic liquid assisted hydrogel functionalized silica stationary phase for mixed-mode liquid chromatography. *Chin. Chem. Lett.* **2025**, *36*, 109889. https://doi.org/10.1016/j.cclet.2024.109889.
143. Liang, C.; Liu, J.; Zhang, H.; et al. Mitigating lipid biofouling in wearable sweat sensors: A study on conductive MOF-based electrodes with tuned hydrophilicity. *Chem. Eng. J.* **2025**, *518*, 164477. https://doi.org/10.1016/j.cej.2025.164477.
144. Wareham-Mathiassen, S.; Jolly, P.; Radha Shanmugam, N.; et al. An Antimicrobial and Antifibrotic Coating for Implantable Biosensors. *Biosensors* **2025**, *15*, 171. https://doi.org/10.3390/bios15030171.
145. Kang, M.; Park, J.; Kim, S.A.; et al. Modulus-tunable multifunctional hydrogel ink with nanofillers for 3D-Printed soft electronics. *Biosens. Bioelectron.* **2024**, *255*, 116257. https://doi.org/10.1016/j.bios.2024.116257.
146. Pan, M.; Shui, T.; Zhao, Z.; et al. Engineered Janus hydrogels: Biomimetic surface engineering and biomedical applications. *Natl. Sci. Rev.* **2024**, *11*, nwae316. https://doi.org/10.1093/nsr/nwae316.
147. Xu, Y.; Sun, K.; Huang, L.; et al. Magneto-induced Janus adhesive-tough hydrogels for wearable human motion sensing and enhanced low-grade heat harvesting. *ACS Appl. Mater. Interfaces* **2024**, *16*, 10556–10564. https://doi.org/10.1021/acsami.3c19373.
148. Zhang, C.W.; Chen, C.; Duan, S.; et al. Hydrogel-based soft bioelectronics for personalized healthcare. *Med-X* **2024**, *2*, 20. https://doi.org/10.1007/s44258-024-00036-0.
149. Sun, Z.; Cao, X.; Wang, S.; et al. Designing polydopamine embedded hydrogel with high-stable adhesion and long-term stability at high temperature. *Polymer* **2025**, *317*, 127914. https://doi.org/10.1016/j.polymer.2024.127914.
150. Lian, Z.; Wang, L.; Jiang, Y.; et al. 3D-printed octopus-inspired PAM/CS hydrogels with excellent adhesion for high-performance ECG sensors. *Chem. Eng. J.* **2025**, *508*, 161043. https://doi.org/10.1016/j.cej.2025.161043.
151. Li, W.; Liu, H.; Mi, Y.; et al. Robust and conductive hydrogel based on mussel adhesive chemistry for remote monitoring of body signals. *Friction* **2022**, *10*, 80–93. https://doi.org/10.1007/s40544-020-0416-x.
152. Shin, Y.; Lee, H.S.; Kim, J.-U.; et al. Functional-hydrogel-based electronic-skin patch for accelerated healing and monitoring of skin wounds. *Biomaterials* **2025**, *314*, 122802. https://doi.org/10.1016/j.biomaterials.2024.122802.
153. Ren, N.; Zheng, G.; Cui, M.; et al. Integrally formed Janus adhesive conductive hydrogel with excellent interfacial stability and fatigue resistance for robust flexible sensing. *Cell Rep. Phys. Sci.* **2025**, *6*, 102916. https://doi.org/10.1016/j.xcrp.2025.102916.
154. Yao, B.; Wu, S.; Wang, R.; et al. Hydrogel ionotronics with ultra-low impedance and high signal fidelity across broad frequency and temperature ranges. *Adv. Funct. Mater.* **2022**, *32*, 2109506. https://doi.org/10.1002/adfm.202109506.
155. Jayakumar, K.; Lielpetere, A.; Domingo-Lopez, D.A.; et al. Tethering zwitterionic polymer coatings to mediated glucose biosensor enzyme electrodes can decrease sensor foreign body response yet retain sensor sensitivity to glucose. *Biosens. Bioelectron.* **2023**, *219*, 114815. https://doi.org/10.1016/j.bios.2022.114815.
156. Zhao, B.; Li, Z.; Zheng, L.; et al. Recent progress in the biomedical application of PEDOT: PSS hydrogels. *Chin. Chem. Lett.* **2024**, *35*, 109810. https://doi.org/10.1016/j.cclet.2024.109810.
157. Conti, S. Robust pure PEDOT: PSS hydrogels for bioelectronic interfaces. *Nat. Rev. Electr. Eng.* **2024**, *1*, 356. https://doi.org/10.1038/s44287-024-00066-1.
158. Wen, J.; Huang, S.; Hu, Q.; et al. Recent advances in zwitterionic polymers-based non-fouling coating strategies for biomedical applications. *Mater. Today Chem.* **2024**, *40*, 102232. https://doi.org/10.1016/j.mtchem.2024.102232.
159. Yadav, S.; Rani, N.; Saini, K.; et al. Biological evaluation of medical devices. In *Medical Devices in Modern Healthcare*, Elsevier: Amsterdam, The Netherlands, 2026; pp. 475–498. https://doi.org/10.1016/b978-0-443-32828-2.00010-7.
160. Stewart, E.M.; Narayan, S.; Anand, L. An electro-chemo-mechanical theory for hydrogel ionotronics: Application to modeling a capacitive strain sensor and a dynamic large strain actuator. *J. Mech. Phys. Solids* **2023**, *173*, 105196. https://doi.org/10.1016/j.jmps.2022.105196.
161. Castillo-Acuna, R.; Kochmann, D.M. Multiphysics modeling of hydrogels with a maximum-entropy-based meshless framework. *Comput. Methods Appl. Mech. Eng.* **2025**, *446*, 118293. https://doi.org/10.1016/j.cma.2025.118293.
162. Xu, Z.; Yue, P.; Feng, J.J. A theory of hydrogel mechanics that couples swelling and external flow. *Soft Matter* **2024**, *20*, 5389–5406. https://doi.org/10.1039/d4sm00424h.
163. Lyu, Z.; Sciazko, A.; Shikazono, N.; et al. Enhanced temporal prediction of electrochemical impedance spectroscopy using long short-term memory neural networks. *Electrochim. Acta* **2024**, *508*, 145227. https://doi.org/10.1016/j.electacta.2024.145227.
164. Wang, Z.; Wang, Y.; Py, B.; et al. DRTtools: Freely Accessible Distribution of Relaxation Times Analysis for Electrochemical Impedance Spectroscopy. *ACS Electrochem.* **2025**, *1*, 2680–2689. https://doi.org/10.1021/acselectrochem.5c00334.

165. Zhu, S.; Jia, G.; Sui, S.; et al. Integrating large language and multimodal models with machine learning for equivalent circuit analysis of electrochemical impedance spectroscopy. *J. Mater. Sci.* **2025**, *60*, 22189–22202. https://doi.org/10.1007/s10853-025-11692-x.
166. Ansari, M.; Darvishi, A. A review of the current state of natural biomaterials in wound healing applications. *Front. Bioeng. Biotechnol.* **2024**, *12*, 1309541. https://doi.org/10.3389/fbioe.2024.1309541.
167. Yuan, W.; Qu, X.; Lu, Y.; et al. MXene-composited highly stretchable, sensitive and durable hydrogel for flexible strain sensors. *Chin. Chem. Lett.* **2021**, *32*, 2021–2026. https://doi.org/10.1016/j.cclet.2020.12.003.
168. Isik, M.; Lonjaret, T.; Sardon, H.; et al. Cholinium-based ion gels as solid electrolytes for long-term cutaneous electrophysiology. *J. Mater. Chem. C* **2015**, *3*, 8942–8948. https://doi.org/10.1039/c5tc01888a.
169. De la Cruz, L.G.; Abt, T.; León, N.; et al. Ice-template crosslinked PVA aerogels modified with tannic acid and sodium alginate. *Gels* **2022**, *8*, 419. https://doi.org/10.3390/gels8070419.
170. Li, M.; Li, W.; Guan, Q.; et al. Sweat-resistant bioelectronic skin sensor. *Device* **2023**, *1*, 100006. https://doi.org/10.1016/j.device.2023.100006.
171. Liu, L.; Feng, X.; Du, J.; et al. Sweat-activated conductive hydrogel nanomesh for breathable, long-term electrophysiological monitoring and human-centric interfaces. *Matter* **2026**, *9*, 102428. https://doi.org/10.1016/j.matt.2025.102428.
172. Zhu, Y.; Chen, B.; Liu, Y.; et al. Recent advances in conductive hydrogels for electronic skin and healthcare monitoring. *Biosensors* **2025**, *15*, 463. https://doi.org/10.3390/bios15070463.
173. Tian, Y.; Yang, Y.; Tang, H.; et al. An implantable hydrogel-based phononic crystal for continuous and wireless monitoring of internal tissue strains. *Nat. Biomed. Eng.* **2025**, *9*, 1335–1348. https://doi.org/10.1038/s41551-025-01374-z.
174. Ding, M.; Xie, P.; Wang, J.; et al. Biomimetic microstructure design for ultrasensitive piezoionic mechanoreceptors in multimodal object recognition. *Nat. Commun.* **2025**, *16*, 8129. https://doi.org/10.1038/s41467-025-63115-9.
175. Ni, Y.; Zang, X.; Yang, Y.; et al. Environmental stability stretchable organic hydrogel humidity sensor for respiratory monitoring with ultrahigh sensitivity. *Adv. Funct. Mater.* **2024**, *34*, 2402853. https://doi.org/10.1002/adfm.202402853.
176. Oh, B.; Lim, Y.-S.; Ko, K.W.; et al. Ultra-soft and highly stretchable tissue-adhesive hydrogel based multifunctional implantable sensor for monitoring of overactive bladder. *Biosens. Bioelectron.* **2023**, *225*, 115060. https://doi.org/10.1016/j.bios.2023.115060.
177. Wang, Y.; Ge, M.; Wang, R.; et al. Injectable ultrasonic metagels for intracranial monitoring. *npj Biosensing* **2025**, *2*, 38. https://doi.org/10.1038/s44328-025-00058-7.
178. Huang, X.; Yang, N.; Sun, S.; et al. Recent progress of hydrogel-based bioelectronics for mechanophysiological signal sensing. *Mater. Sci. Eng. R Rep.* **2025**, *162*, 100888. https://doi.org/10.1016/j.mser.2024.100888.
179. Sagdic, K.; Fernandez-Lavado, E.; Mariello, M.; et al. Hydrogels and conductive hydrogels for implantable bioelectronics. *MRS Bull.* **2023**, *48*, 495–505. https://doi.org/10.1557/s43577-023-00536-1.
180. Amoli, V.; Kim, J.S.; Jee, E.; et al. A bioinspired hydrogen bond-triggered ultrasensitive ionic mechanoreceptor skin. *Nat. Commun.* **2019**, *10*, 4019. https://doi.org/10.1038/s41467-019-11973-5.
181. Zheng, Y.; Wang, J.; Cui, T.; et al. Transparent ionogel balancing rigidity and flexibility with prolonged stability for ultra-high sensitivity temperature sensing. *Chem. Eng. J.* **2024**, *494*, 152695. https://doi.org/10.1016/j.cej.2024.152695.
182. Zheng, Y.; Liu, H.; Wang, J.; et al. Unlocking intrinsic conductive dynamics of ionogel microneedle arrays as wearable electronics for intelligent fire safety. *Adv. Fiber Mater.* **2024**, *6*, 195–213. https://doi.org/10.1007/s42765-023-00344-x.
183. Huang, W.; Ding, Q.; Wang, H.; et al. Design of stretchable and self-powered sensing device for portable and remote trace biomarkers detection. *Nat. Commun.* **2023**, *14*, 5221. https://doi.org/10.1038/s41467-023-40953-z.
184. Yang, M.; Hu, Y.; Wang, X.; et al. Chaotropic Effect-Boosted Thermogalvanic Ionogel Thermocells for All-Weather Power Generation. *Adv. Mater.* **2024**, *36*, 2312249. https://doi.org/10.1002/adma.202312249.
185. Li, M.; Guan, Q.; Li, C.; et al. Self-powered hydrogel sensors. *Device* **2023**, *1*, 100007. https://doi.org/10.1016/j.device.2023.100007.
186. Ou, K.; Wang, M.; Meng, C.; et al. Enhanced mechanical strength and stretchable ionic conductive hydrogel with double-network structure for wearable strain sensing and energy harvesting. *Compos. Sci. Technol.* **2024**, *255*, 110732. https://doi.org/10.1016/j.compscitech.2024.110732.
187. Zhang, Y.; Wang, H.; Khan, S.A.; et al. Deep-learning-assisted thermogalvanic hydrogel fiber sensor for self-powered in-nostril respiratory monitoring. *J. Colloid Interface Sci.* **2025**, *678*, 143–149. https://doi.org/10.1016/j.jcis.2024.09.132.
188. Wang, X.; Yuan, G.; Zhou, H.; et al. Composite laminar membranes for electricity generation from water evaporation. *Nano Res.* **2024**, *17*, 307–311. https://doi.org/10.1007/s12274-023-5906-5.
189. Chen, J.; Zhang, X.; Cheng, M.; et al. A self-sustained moist-electric generator with enhanced energy density and longevity through a bilayer approach. *Mater. Horiz.* **2025**, *12*, 2309–2318. https://doi.org/10.1039/d4mh01642d.
190. Chang, K.; Zhang, C.; Liu, T. A comprehensive review on fabrication and structural design of polymer composites for wearable pressure sensors. *Polym. Sci. Technol.* **2025**, *1*, 3–24. https://doi.org/10.1021/polymscitech.4c00047.